Research paper

i. Title

Geographic and subsequent biotic isolations led to a diversity anomaly of section *Heterotropa* (genus *Asarum*: Aristolochiaceae) in insular versus continental regions of the Sino-Japanese Floristic Region

ii. Running title

Abiotic and biotic isolations in *Heterotropa*

iii. The names of authors

Daiki Takahashi[1*], Shota Sakaguchi[1], Yu Feng[2], Yuji Isagi[3], Ying-Xiong Qiu[2], Pan Li[2], Rui-Sen Lu[2], Chang-Tse Lu[4], Shih-Wen Chung[5], Yang-Shan Lin[6], Yun-Chao Chen[6], Atsushi J. Nagano[7], Lina Kawaguchi[7], Hiroaki Setoguchi[1]

iv. Authors' affiliations

[1]Graduate school of Human and Environmental studies, Kyoto University, Japan; [2]Systematic & Evolutionary Botany and Biodiversity Group, MOE Laboratory of Biosystem Homeostasis and Protection, College of Life Sciences, Zhejiang University, China; [3]Graduate school of Agriculture, Kyoto University, Japan; [4]Department of Biological Resources, National Chiayi University, Taiwan; [5]Herbarium of Taiwan Forestry Research Institute, Taiwan; [6]Miaoli Distinct Agricultural Research and Extension station, Taiwan; [7]Faculty of Agriculture, Ryukoku University, Japan

*Correspondence: Daiki Takahashi, Graduate school of Human and Environmental studies, Kyoto University, Yoshida-Nihonmatsu-cho, Sakyo-ku, Kyoto, Japan

v. Acknowledgements

We are fully grateful to the editor and reviewers for their helpful comments on our paper. We also thank S. Gale, S. Liao, K. Maeda, J. Nagasawa, S. Nemoto, T. Teramine, M. and S. Zhou for their help with sampling. We are also grateful to J. R. P. Worth, and M. Yamasaki for their valuable comments on the statistical analyses and manuscript writing. This work was supported by Grants-in-Aid for Scientific Research from the Japan Society for the Promotion of Science (Nos. 24247013, 26304013 and 18J22919), the Environment Research and Technology Development Fund (grant no. 4-1702 and 4-1902), and the Environmental Research and Technology Development Fund of the Ministry of the Environment SICORP Program of the Japan Science and Technology Agency (grant no. 4-1403). Permits were note required in this study.

vi. Abstract and keywords

Aim

The Sino-Japanese Floristic Region has extremely high species diversity with respect to temperate plants; however, the reasons for this diversity are poorly under- stood because most studies have only considered geographic isolation caused by climatic oscillations. In some plant groups, high floral trait diversity and uneven species diversity between insular systems and the continental area suggest other factors may have important roles too. The primary purpose of this study is to reveal how abiotic and biotic factors have shaped the species diversity anomaly of *Heterotropa* between the insular systems and the continental area. Location: The Sino-Japanese Floristic Region. Taxon:

Location

The Sino-Japanese Floristic Region

Taxon

Section *Heterotropa* (genus *Asarum*; Aristolochiaceae)

Methods

Using ddRAD-seq and chloroplast genome data, we built a time-calibrated phylogenetic tree including 79 species. We estimated the patterns of floral traits (flowering time and floral size) evolution using macroevolutionary modelling, and tested the correlation of speciation rate with the trait evolution rates. Finally, we estimated the isolation factors of all taxa pairs and sister-taxa pairs based on distribution range and floral traits.

Results

Phylogenetic analysis indicated that *Heterotropa* was diverged into two clades (continental clade and insular clade) in the Miocene, and the major subclades corresponded to geographic entities. Most rate shifts accelerating floral trait's evolution occurred during the Pleistocene period. Evolution rate of floral traits showed positive correlation with the speciation rate. Large proportion of taxa in the insular clade are distributed allopatrically. Several sister pairs showed floral trait divergence with geographic overlap.

Main conclusions

The diversification of *Heterotropa* appears to have been triggered by geographic and climatic events, and subsequent repeated floral trait evolution with and without geographic isolation. Furthermore, the high species diversity in the insular systems would have been formed by the repeated range fragmentations and contractions. Our study demonstrates the importance of multidimensional studies to understand the diversification process of temperate plants in the Sino- Japanese Floristic Region.

Keywords

Asarum sect. *Heterotropa*, diversity anomaly, East Asia, island biogeography, macroevolutionary modelling, morphological evolution, phylogenetics

vii. Main text

1. Introduction

The Sino-Japanese Floristic Region (SJFR) extends from the eastern Himalayas to the Japanese Archipelago through south and central China (Wu & Wu, 1996). This region boasts one of the most diverse temperate floras anywhere in the world and has high endemism (Wu & Wu, 1996). This diversity has been thought to be linked to climatic and physiographical complexity and historical environmental changes associated with the Pleistocene (< 2.6 Mya) climatic oscillations (Qian & Ricklefs, 2000). During glacial periods, when the climate of this region was cooler by ca. 4-6 °C and sea level was approximately 130m lower than its present level, temperate plants in this region retreated to refugia at lower altitudes or southern parts (Harrison, Yu, Takahara, & Prentice, 2001). During the interglacial periods, expansion to higher altitudes or northern parts would have occurred. In the eastern island systems, sea level changes due to climatic oscillations have caused repeated formation and division of land-bridges in the East China Sea (Ujiie, 1990) and these events have provided opportunities for population expansion and fragmentation (Qiu, Fu, & Comes, 2011). Many phylogeographic studies have revealed that the present interspecific and intraspecific genetic structures of temperate plants in this region reflected the range shifts caused by climatic oscillations (reviewed in Qiu et al., 2011). It has been considered that these climatic and associated environmental changes during the Pleistocene period triggered range fragmentation, vicariance, and population isolation (Qiu et al., 2011). Therefore, allopatric speciation could be a major mode of speciation in the temperate plants of this region (Qian & Ricklefs, 2000).

Although the importance of geographic isolation as a major isolation mechanism in plants has been addressed (Boucher, Zimmermann, & Conti, 2016), recent studies in other regions have implied that biotic factors also promote species diversification (Lagomarsino, Condamine, Antonelli, Mulch, & Davis, 2016). In particular, floral trait evolution has been thought to promote speciation through segregation of gene flow by pollinator shifts (Armbruster, 2014). Previous studies have shown that the tempo and pattern of floral trait evolution varies

distinctively among lineages, and floral trait evolution has been implicated in shaping patterns of species diversification (Givnish et al., 2015; Jaramillo & Manos, 2001). This implies that biotic factors can play complementary roles to abiotic factors in reproductive isolation; that is, biotic factors can facilitate reproductive isolation even without geographical isolation (Rundle & Nosil, 2005). To fully understand the diversification process of species groups, it is essential to reveal the relative contributions of biotic and abiotic factors. However, many studies conducted in the SJFR have only discussed the role of allopatric fragmentation due to geographic and climatic events, and few studies have considered other factors as drivers of the diversification of the temperate plants. In addition, most phylogeographic studies in the region have focused on individual species or only small groups, including fewer than 10 taxa (but Mitsui, Nomura, Isagi, Tobe, & Setoguchi, 2011; Yoichi, Jin, Peng, Tamaki, & Tomaru, 2017). Thus, our knowledge of the diversification process of temperate plants in the SJFR remains fragmentary, due to a lack of integrative multidimensional studies of morphology, phylogeny, biogeography, and ecology with adequate sampling of diversified groups.

In this study, we focused on the section *Heterotropa* (genus *Asarum*; Aristolochiaceae), one of the most speciose warm-temperate plant groups (comprising approximately 90 species) endemic to the SJFR (Sugawara, 2006). Taxa of *Heterotropa* are rhizomatous herbs that grow in shaded understories, and are distributed in mainland China (25 species), Taiwan (13 species), and the Japanese archipelago, including the Ryukyu islands (50 species). The species diversity of *Heterotropa* is uneven, and given the difference in areas, *Heterotropa* shows a species diversity anomaly; higher in the eastern insular region and lower in the continental area (from Taiwan to mainland Japan; 2.7×10^{-4} species/km^2 and mainland China; 1.3×10^{-5} species/km^2, see Results). Some taxa of *Heterotropa* have very limited geographic ranges (e.g., in only one island or mountain range), and the dispersal ability of *Heterotropa* is estimated to be 10 – 50 cm per year due to its myrmecochore seeds with elaiosome (Hiura, 1978). Low dispersal ability promotes genetic differentiation among populations and often leads to allopatric speciation (Petit et al., 2005). These confined distribution ranges and the low dispersal ability led us to hypothesise an allopatric speciation process for *Heterotropa*. On the other hand, *Heterotropa*

taxa are characterised by high divergence in floral traits, in terms of their shapes, sizes, and colours of calyx tubes and lobes (Fig. 1a & S1), while their vegetative traits show almost no differences (Sugawara & Ogisu, 1992). The sepals connect beyond attachment to the ovary and form a calyx tube with calyx lobes (Sugawara, 1987), and their flowers have been hypothesised to mimic fungi in order to attract fungus gnats (Sinn, Kelly, & Freudenstein, 2015). In addition to flower shape, *Heterotropa* taxa are highly divergent in flowering time; most taxa have flowers in spring, while others have flowers in autumn or winter (Sugawara, 2006). A genus-wide phylogenetic study of *Asarum* showed that diversification of *Heterotropa* could have been triggered by the presence of putative fungal-mimicking floral structures, loss of autonomous selfing, and loss of vegetative reproduction (Sinn et al., 2015). Given these characteristics, we considered that *Heterotropa* would be an ideal subject for investigating the relative importance of abiotic and biotic effects on its diversification in the SJFR. Our previous phylogenetic study using the ITS region showed that *Heterotropa* was monophyletic and comprised two clades, which corresponded to geographic patterns, namely mainland China and the island arc from Taiwan to mainland Japan (Takahashi & Setoguchi, 2018). Furthermore, Okuyama et al., (2020) divided Japanese *Heterotropa* into nine groups by phylogenetic analysis using RAD-seq datasets including 47 insular and 5 continental species. However, due to the low resolution of the datasets or lack of inclusive sampling around the SJFR, the formation mechanisms of the high species diversity in the insular systems and their diversification history in terms of temporal and spatial patterns of floral trait evolution remain unknown.

Our primary purpose in this study was to reveal the diversification history of *Heterotropa* taxa in the SJFR, especially focusing on the relative contribution of abiotic and biotic drivers and the species diversity anomaly between the insular systems and the continental area. The following specific questions were addressed; (1) Did speciation events in *Heterotropa* mainly occur during the Pleistocene period, when the climatic and environmental changes would have triggered population fragmentation and expansion of temperate plants in the SFFR? (2) Did repeated formation and division of land-bridges in the East China Sea promote dispersal or isolation of insular taxa? (3) Are rates of floral trait evolution correlated with the speciation

rate in *Heterotropa*, showing diverse floral morphology and phenology? (4) Which is major isolation factor in sister-taxa pairs, non-overlap of distribution range or differentiation of floral traits? Understanding the relative roles of biotic and geographic factors that have shaped species diversity across space and time provides insights into the diversification process of temperate plants in the SJFR.

2. Materials and methods

2.1 *Taxon sampling*

Here, we sampled 79 *Heterotropa* species throughout the distribution range of the section (Fig 1b, Table S1), including three undescribed but morphologically distinct taxa (*Asarum kiusianum* var. *tubulosum* nom. nud. [Maekawa, 1983], *A. tarokoense* nom. nud. [Lu et al., in prep.], and *A. titaense* nom. nud. [Setoguchi et al., in prep]). *A. satsumense* has been considered to be distributed in both Taiwan and Kyushu islands (Lu, Chiou, Liu, & Wang, 2010), and our preliminary examination suggested that the Taiwanese entity should be distinguished from the species (Lu and Takahashi, personal observation). Thus, in this study, we treated *A. satsumense* collected from the Taiwan and Kyushu islands as a different taxon (*A. satsumense* W; Taiwanese and *A. satsumense* K; Japanese). The sample set included 46 Japanese species (52 taxa), 13 Taiwanese species (13 taxa), and 20 mainland Chinese species (20 taxa). As an outgroup species, we used one section *Hexastylis* species (*A. shuttleworthii*) according to our previous study (Takahashi & Setoguchi, 2018).

2.2 *Sequencing and phylogenetic analysis*

For phylogenetic analysis, we adopted hierarchical calibration methods using different datasets (chloroplast CDS regions and ddRAD-seq). We firstly conducted phylogenetic analysis of 59 CDS regions obtained from chloroplast genome data (Table S2 & S3) and estimated the divergence time of *Heterotropa* using the crown age of Magnoliid. Then, we constructed time-calibrated phylogenetic trees of ddRAD-seq data of 85 *Heterotropa* taxa with *A. shuttleworthii* using the obtained crown age of *Heterotropa*. Details of library preparation, sequencing methods, data processing and phylogenetic analysis are described in Appendix 1.

2.3 *Ancestral area reconstruction*

To infer the ancestral areas and phylogeographic history of *Heterotropa* taxa, we performed statistical dispersal-vicariance analysis (S-DIVA) using RASP v3.2 (Yu, Harris, & He, 2010).

The maximum number of areas was constrained to 2, but we also explored the importance of changing the maximum areas (setting number of maximum areas = 3, and 4). To accommodate phylogenetic uncertainty, the analysis was conducted using 1000 phylogenetic trees of the ddRAD-seq dataset obtained from BEAST. We divided the distribution range of *Heterotropa* into seven regions: (A) Sichuan basin and surrounding mountains, (B) other parts of mainland China, (C) Taiwan and southern Ryukyu islands, (D) central Ryukyu islands, (E) northern Ryukyu islands and Kyushu island, (F) southern part of mainland Japan including Shikoku island, and (G) northern part of mainland Japan (see Fig. 1c). The boundaries of these regions were defined with reference to biogeographic studies (e.g., C and D; Kerama gap, D and E; Tokara gap [Kimura, 1996], F and G; Itoigawa-Shizuoka tectonic line [Okamura *et al*., 2017]) and phylogeographic studies (Landrein, Buerki, Wang, & Clarkson, 2017). Most species used in this study are distributed in one region and only three species (*A. asperum*, *A. nipponicum* and *A. maximum*) are distributed across two regions.

2.4 *Analysis of floral trait evolution*

To test whether biotic factor affected the diversification of *Heterotropa*, we investigated patterns of floral trait evolution and correlations between rates of speciation and trait evolution. As objected traits, we focused on flowering time and calyx tube width. Flowering time is related to the local environment, including pollinator fauna, and its differences play a role in the reproductive barrier among taxa. Calyx tube width would be linked to pollinator size selection and its difference could affect the difference in pollinator fauna, which leads to reproductive isolation. The data collection methods were described in Appendix 1.

To estimate evolutionary rates and rate shifts of floral trait evolution on the phylogenetic tree of *Heterotropa*, we conducted Bayesian macroevolutionary analysis for flowering time and calyx tube width implemented in BAMM v. 2.5.2 (Rabosky, 2014). BAMM models shift in macroevolutionary regimes across a phylogenetic tree using reversible-jump Markov chain Monte Carlo (rjMCMC) sampling. Because BAMM analysis can only treat continuous characters, we transformed the flowering time to the scaled values (Fig S2), where

October is set as 1, November as 2, December as 3, January as 4, February as 5, March as 6, April as 7 and May as 8. The prior values were set using "BAMMtools" package (Rabosky et al., 2014) for R v. 3.5.4 (R Core Team, 2013), and the analysis was conducted using a maximum clade credibility tree obtained from BEAST. To ease model complexity, we adopted the time-invariant Brownian motion model of trait evolution. The analysis involved a rjMCMC run of 10,000,000 generations sampled every 10,000 steps, and the initial 3,000,000 generations were discarded as burn-in. The rjMCMC convergence was confirmed using BAMMtools. To infer the location of rate shifts, we calculated the marginal odds ratios on individual branches (Shi & Rabosky, 2015). Then, to infer the difference of evolutionary rates among clades, we reported the mean scaled tree of trait from the outputs of BAMM, in which each branch length is shortened or stretched proportional to the model-averaged mean evolutionary rates of the traits. We reported the top four most credible shift distributions for each trait. Finally, to infer the temporal change in traits' evolution rates, we plotted the evolutionary rate variation through time for each trait and clade.

To investigate correlation between the rates of speciation and trait evolution, we first fitted BAMM speciation rate model and inferred per-lineage rates of speciation. The analysis setting was same as we performed for estimating trait evolution rates, but MCMC run length was 5,000,000 and sampling frequency was set to 5,000. Per-lineage rates of trait evolution for each trait were obtained from the BAMM results. Average rates of speciation and trait evolution for each blanch were extracted by using "getMeanBranchLengthTree" function in BAMMtools. For inferring the significance of correlation between the rates, we fitted phylogenetic generalized least square (PGLS) model using "phylolm" package (Ho et al., 2016). Subsequently, we applied a simulation-based test (Cor-STRATES; Cooney & Thomas, 2021), which compares the observed correlation between rates with a null set of correlations generated by simulation. It was reported that Cor-STRATES showed lower type I error rates and exhibited higher statistical powers compared with PGLS method (Cooney and Thomas, 2021). In order to conduct Cor-STRATES test, we fitted Brownian motion (BM) model to each observed trait data (flowering time and calyx tube width) and estimated the value of the diffusion rate (σ^2)

parameter using "geiger" package (Harmon, Weir, Brock, Glor, & Challenger, 2008). We performed 200 simulations based on a BM null model utilizing the estimated σ^2 and obtained sets of null trait data for each trait. We then re-estimated per-lineage rates of trait evolution for each null trait dataset by using BAMM, and calculated Spearman's rank correlation coefficient (ρ) between observed speciation rate and trait evolution rate for each null simulation. By using the script in Cooney and Thomas (2021), we computed a two-tailed *P* value for the observed correlation.

2.5 *Geographic overlap within each clade*

The potential geographic range of each taxon was set by creating a convex polygon from the distribution data. Distribution data for all taxa were based on the specimen records of the herbarium of Kyoto University (KYO), S-Net data portal (http://science-net.kahaku.go.jp/, accessed on 2019/1/26), and the Chinese Virtual Herbarium (http://www.cvh.org.cn/, accessed on 2019/1/26), and results of personal observations. Because the distribution range of many *Heterotropa* taxa tends to be confined to a small area, we considered that setting any threshold values of the number of records would exclude local endemics from the dataset. Thus, we didn't set any threshold values to make distribution data. In total, we collected 1396 occurrences for 84 taxa (minimum 1, maximum 197; Table S1). We were not able to find available records for *A. nobillisimum* and excluded this taxon from the analysis. A single convex polygon for each taxon was created by connecting the outline of the occurrence point(s) by placing a 1 km round buffer and masking by a costal line. We have compared our estimated distribution areas with the distribution ranges shown in Kishi & Irizawa, (2008), which was edited by horticultural experts of *Asarum*, and confirmed that the constructed distribution ranges would be correct. Following Anacker and Strauss (2014), we calculated range overlap as the area occupied by both taxa divided by that of the smaller ranged taxa. The range overlap value ranged from 0 (no overlap) to 1 (complete overlap) and was calculated for all pairs of taxa respectively within each major clade (mainland China, Ryukyu-Taiwan, and mainland Japan clades, see Results section). All geographic analysis were conducted by using "sf" package (Pebesma, 2018) in R.

2.6 *Geographic and morphological isolation*

To infer speciation modes of the insular and the continental clades, we calculated geographic and morphological isolation values of sister taxa. We selected sister pairs with posterior probabilities of nodes higher than 80% in the phylogenetic analysis of ddRAD-seq data sets as sister taxa. The geographic isolation index was calculated by transforming the geographic overlap value into binary data (0; overlap, 1; non-overlap). We set the value of the geographic isolation index of partially overlapping pairs to 0. We also calculated the morphological isolation indices for two floral traits (flowering time and calyx tube diameter) between taxa pairs. To estimate the differentiation of the floral traits, we set the intervals of the traits using the first and last flowering months, and the maximum and minimum values of calyx tube diameters, respectively, according to the trait data. For each trait, when a pair of taxa had an overlap of the intervals, they were scored as 0 for "overlapping"; if they showed no overlap, they were scored as 1 for "divergent". In addition, we measured the geographic and morphologic isolations between all pairs of taxa within the major clades and estimated conditional relationships among the attributes. Although present isolation would not completely link with the speciation events, this could enable us to discuss the trends of isolation factors between the insular and the continental clades.

365

366 **3. Results**

367 **3.1 *ddRAD-seq data***

368 After filtering low-quality reads and bases, the number of ddRAD-seq reads of each sample
369 ranged from 510,135 to 2,558,859 reads and the average number of reads was 1,348,526 (Table
370 S1). Our 50% genotyped matrix consisted of 469 loci, which contained 3,415 parsimony-
371 informative SNPs. Our 70% and 90% matrices included 117 and 46 loci with 710 and 266
372 parsimony informative SNPs, respectively.

373

374 **3.2 *Phylogenetic inference and ancestral area reconstruction***

375 Phylogenetic analysis based on 59 chloroplast CDS regions supported all clades within the tree
376 with posterior probabilities > 0.99 and showed that the *Heterotropa* was monophyletic (Fig.
377 S3). The estimated divergence time between a mainland China taxon and the insular clade
378 including *A. forbesii* was 9.16 Mya (95% HPD: 4.66 - 13.55 Mya).

379 Phylogenetic analysis with 50% genotyped ddRAD-seq matrix yielded strongly
380 supported clades within *Heterotropa* (Fig. 1c). Within the *Heterotropa* clade, the mainland
381 China clade diverged first, followed by a splitting off of *A. forbesii*, which is distributed in
382 mainland China, and the clade that consisted of insular taxa with only one mainland Chinese
383 taxon (*A. ichangense*). Within the insular and the mainland Chinese clades, there were subclades
384 that corresponded with the geographic entities. The mainland China clade was divided into two
385 subclades, including the taxa distributed around the Sichuan basin and in other parts of
386 mainland China. The insular clade consisted of two subclades, including taxa distributed in the
387 southern parts of the Japanese island arc (from Taiwan to the Amami islands; Ryukyu-Taiwan
388 clade) and northern parts (from Tokara islands to Honshu; mainland Japan clade). *A. ichangense*
389 was included in the Ryukyu-Taiwan clade. Within the mainland Japan clade, almost all taxa
390 found on Kyushu island (except for *A. minamitanianum* and *A. asperum*) formed a clade with
391 *A. lutchuense* and *A. curvistigma*, which are found on Amami islands and Honshu island,
392 respectively. The other taxa in mainland Japan clade split into two subclades, both of which

included southern and northern Japanese taxa. All clades mentioned above showed high support (posterior probabilities > 99%) and diverged during the pre-Pleistocene periods (> 2.6 Mya; Fig. S4).

Our BI trees inferred from 75% and 90% genotyped ddRAD-seq matrices also supported the hypothesis that *Heterotropa* split into the insular and mainland China clades, while the nested structures were not resolved (Fig. S5). The tree obtained from the 50% genotyped matrix showed relatively high support of nodes (mean posterior probabilities = 91.0%), while other matrices showed lower supports (75% genotyped matrix; 77.7%, and 90% genotyped matrix; 63.2%). Thus, we adopted the 50% genotyped tree for further analyses.

The results of S-DIVA analysis with setting maximum areas = 2 (Fig. 1c) showed that the origin of *Heterotropa* was in the mainland China region (B) and that dispersal to the insular systems occurred subsequently, while the results with other settings (maximum areas = 3 or 4) failed to support this scenario (Fig. S6). From the insular systems, only one back-dispersal to mainland China was estimated (*A. ichangense*). In the mainland Japan clade, several taxa colonised the northern part of Japan (G) from the southern part (E and F). These events were supported regardless of the number of maximum areas.

3.3 *Analysis of trait evolution*

Most *Heterotropa* taxa (55 taxa) start flowering in spring, whereas 11 taxa flower in autumn and 19 taxa in winter. These autumn-flowering and winter-flowering taxa were scattered across all three major clades (Fig. 2a), implying that the flowering time of *Heterotropa* changed several times in each of the three major clades, especially in tip nodes or branches. The taxa that have more than 15 mm of calyx tube width were observed in the three major clades (Fig. 2b), and the changes would have evolved in parallel.

The results of BAMM analysis showed that for both traits, a single macroevolutionary rate was unlikely to fit our genetic data (Fig. S7), indicating that several rate shifts of trait evolution would have occurred in *Heterotropa.* The marginal odds ratios showed that for both traits, shifts accelerating the trait evolution were distributed across all three major clades (Fig.

2a-1 & 2b-1). Clades with high trait evolution rates indicated that states of the trait would have changed repeatedly within the clades. Most of them were located at internal branches within the regional lineages and occurred during the Pleistocene periods. For both traits, clades with relatively high evolutionary rates contained only several taxa (Fig. 2a-2 & 2b-2). As an exception, the clade containing 16 mainland Japanese taxa and that containing nine mainland China taxa showed high evolutionary rates of flowering time. These tendencies were supported in the top four credible shift distributions (Fig. S8 & S9). Furthermore, in the regards of flowering time, the results of ancestral state reconstruction analysis also supported that traits changes would have occurred across all three clades and especially within the clades containing several taxa (Fig. S10). Rate variation through time plots indicated that the evolutionary rates of both traits increased in all clades through time, and although their 95% CIs were overlapped, the rates of flowering time in the mainland Japan clade was higher than other clades (Fig. S11).

PGLS analysis showed positive relationships between the rates with relatively low *P* values (PGLS slope = 1.43e-4, $P = 0.139$ for flowering time, and PGLS slope = 4.85e-5, $P = 0.023$ for calyx tube width). Furthermore, Cor-STRATES test showed that each trait evolution rate was positively correlated with the speciation rate ($\rho = 0.208$ and $P = 0.050$ for flowering time, and $\rho = 0.197$ and $P = 0.030$ for calyx tube width; Fig. 3), indicating that the evolution of both traits would have been concerned with the diversification of *Heterotropa*.

3.4 *Geographic and floral trait isolation*

The mean values of the distribution areas of the taxa within mainland China, Ryukyu-Taiwan, and mainland Japan clades were 172,168 km^2, 570 km^2, and 6,524 km^2, respectively, (Table S1; Fig S12). Within these clades, most pairs were distributed allopatrically (Table 1; Fig. S13abc). The mainland China clade contained a relatively low proportion of geographically isolated pairs (69.85%), followed by the Ryukyu-Taiwan clade (88.60%), and mainland Japan clade (90.36%).

Eleven sister pairs out of 24 pairs showed geographic overlap to various degrees (17 - 100%), and seven sister-pairs showed more than 80% range overlap (Table 2 & Fig. S13d). In the continental clade, four sister-pairs out of five pairs showed range overlap, while in the

insular clade, only seven sister pairs out of 18 pairs showed range overlap. We found 14 sister pairs showing divergence based on either flowering time or calyx tube diameter. Six sister-pairs showed floral trait divergence with geographic overlap.

Within the mainland Japan clade, 52.44% of taxon pairs showed divergence in flowering time, whereas the proportion of taxon pairs showing divergence in calyx tube diameter was lower (36.28%). Conversely, both Ryukyu-Taiwan and mainland China clades contained relatively high proportions of taxa pairs showing divergence in calyx tube diameter (56.13% and 68.63%, respectively), while only 21.37% and 28.76% of taxa pairs showed divergence in flowering time, respectively. All three clades included a high proportion of taxa pairs that differentiated in either flowering time or calyx tube diameter (mainland Japan: 71.02%, Ryukyu-Taiwan: 66.76%, and mainland China: 76.47%). In all three clades, most pairs showing floral trait differentiation were geographically isolated, that is, there were no conditional relationships between geographic overlap and floral trait differentiation (Fig. 4).

4. Discussion

4.1 *Phylogeographic history of* Heterotropa *in the SJFR*

Heterotropa was estimated to be originated in mainland China (Fig. 1), and the divergence time between the continental and the insular clades estimated from the chloroplast phylogenetic analysis was 9.16 Mya, corresponding to the late Miocene period (Fig. S3). These results were concordant with our previous study using the average substitution rate of the ITS region (9.3 Mya; Takahashi & Setoguchi, 2018). During the late Miocene period, regressions and transgressions of the East China Sea (Haq, Hardenbol, & Vail, 1987) caused land-bridge formation that may have allowed the migration and divergence of temperate plants between the mainland China and the insular systems (Qi et al., 2012; Yang et al., 2017). Furthermore, our study revealed that besides the insular clade, the mainland China clade was also composed of subclades, which corresponded to geographic entities (Fig. 1), and all subclades diverged during the late Miocene or the Pliocene periods (Fig. S4). During these periods, the establishment of a monsoon climate caused by the uplift of the Himalayas and the Tibetan Plateau led to vegetational shifts in the SJFR, and frequent glacial-regressions and inter-/after-glacial transgressions (Kimura, 1996). We considered that geographic and climatic events would have allowed formation of the regional lineages of *Heterotropa,* as shown in other studies (Mitsui et al., 2008; Yang et al., 2017).

As an exception, two Chinese species were not included in the mainland China clade: *A. forbesii* and *A. ichangense* were sister to or included in the insular clade. The phylogenetic placement of the two species is consistent with a previous phylogenetic study (Okuyama et al., 2020) and the chromosomal study that showed they have the same chromosome numbers (2n = 24) as insular taxa, which is different from the other mainland China species (2n = 26) (Sugawara & Ogisu, 1992). Our study using exclusive sampling of Chinese taxa demonstrated that only one back dispersal event from the insular systems to mainland China would have occurred. In addition, colonisation to other regions after formation of the regional lineages was observed only in few taxa (e.g., *A. minamitanianum* from mainland Japan to Kyushu island).

505 This indicated that the regional lineages would have remained separated during the Pleistocene
506 period. One of the reasons would be glacial isolation. In the SJFR, the existence of multiple
507 refugia of temperate plants is implied by phylogeographic studies (Qiu et al., 2011). In mainland
508 China, in addition to southern areas (< 30°N), several refugia would have been located around
509 the Sichuan basin, and this region would have been isolated from other regions due to its
510 complex topography, including high mountains and the Yangtze River (Wang et al., 2015). In
511 mainland Japan, during the glacial periods, most parts were covered by mixed (boreal and cool
512 temperate) forests or boreal forests (Harrison et al., 2001), and warm temperate plants would
513 have been forced to retreat southward and survive separately in narrow glacial refugia on the
514 southern coasts of Kyushu, Shikoku, and Honshu islands (Aoki et al., 2019). Another isolating
515 factor would be the seaway barriers. In the Ryukyu islands, two deep-water passages (Tokara
516 Tectonic Strait and Kerama gap, currently > 1000m in depth), were formed during the Pliocene
517 period (Kimura, 1996). These deep-water passages act as isolation barriers for plant expansion
518 (Nakamura, Suwa, Denda, & Yokota, 2009). We considered that these glacial and geographic
519 isolations would prevent the colonisation of most *Heterotropa* taxa to other regions.
520
521 **4.2 *Diversity anomaly and its driving forces***
522 Our phylogenetic analysis showed that within *Heterotropa*, most of the speciation events would
523 have occurred during the Pleistocene period (Fig. S4). Compared with continental taxa, insular
524 taxa have smaller distribution ranges (Fig. S12), and a large proportion of insular pairs show
525 geographic isolation (Table 1 & 2). These results likely reflect the repeated range
526 fragmentations and contractions of insular taxa. It has been reported that the repeated exposure
527 and submergence of the land-bridges during the Pleistocene period led to significant population
528 isolations and declines of temperate plants especially in insular systems (Qiu et al., 2011).
529 Furthermore, during glacial periods, warm temperate forests were fragmented in the Japanese
530 archipelago, while the vast areas of central to southern mainland China were covered by them
531 (Harrison et al., 2001). Thus, these geographic and climatic effects would have triggered the
532 divergence of insular *Heterotropa*.

The results of trait evolutionary analyses indicated that the evolutionary rates of both traits increased through time (Fig. S11). In addition, most of the accelerating rate shifts occurred after the formation of regional lineages during the Pleistocene period (Fig. 2). Higher evolutionary rate of flowering time in mainland Japan clade was implied (Fig. S11). The warm temperate forests of mainland Japan are thought to have experienced the significant population declines during the Pleistocene period (Aoki et al., 2019). The morphological heterogeneity would have been facilitated by geographic isolation due to the Pleistocene climatic oscillations as shown in Gao, Zhang, Gao, & Zhu (2015). The random genetic drift associated with the range contractions could be one of the mechanisms of trait evolution in plants (Lande, 2000), and a simulation study also implied that a small population size would promote floral evolution, including flowering time without selective agents (Devaux & Lande, 2008). The range fragmentations during the Pleistocene period would have also led to the floral trait differentiation of *Heterotropa*.

Did the biotic factors contribute to the diversification of *Heterotropa*? In general, floral morphology has been largely interpreted as the historical outcome of pollinator mediated selection (Fenster, Armbruster, Wilson, Dudash, & Thomson, 2004). The pollinator-mediated diversification of *Heterotropa* has been hypothesised in a previous study (Sinn et al., 2015). Empirical studies have implied that the various Diptera species are pollinators of insular *Heterotropa* taxa with specialisation (e.g., fungus gnus in *A. tamaense* [Sugawara, 1988], sciarid flies in *A. costatum* [Kakishima and Okuyama, 2018], and Calliphoridae flies in *A. fudsinoi* [Maeda, 2013]). The floral traits of *Heterotropa* would be related to the attraction of Diptera species, and the pollinator specialization would lead to the formation of prezygotic isolation. Our Cor-STRATES test showed that evolution rates of both traits were significantly correlated with the speciation rate (Fig. 3). Thus, although at present, most taxa pairs are distributed allopatrically (Fig. 4), we considered that besides abiotic factors, biotic factors are likely to affect the diversification of *Heterotropa*.

4.3 *Biotic and abiotic drivers of sister taxa divergence*

We found 11 sister-pairs show geographic overlap (seven pairs in the insular clade, and four in the continental clade), indicating that, besides allopatric speciation, speciation on a small spatial scale could have also occurred. Geographical overlap between close relatives requires some kind of reproductive isolation to maintain the species boundary (Weber & Strauss, 2016). Six geographically overlapping sister taxa pairs showed floral trait differentiation (Table 2). In *Heterotropa*, most taxa inhabit almost the same environments (understory of warm temperate forests) and the floral difference and/or geographic isolation would act as reproductive barriers rather than habitat differences. This insight was corroborated in a study of nine closely related *Heterotropa* taxa in the Amami islands, which are distributed in sympatry and/or close parapatry and morphologically different in floral traits (Matsuda, Maeda, Nagasawa, & Setoguchi, 2017). Thus, we considered that the divergence in flowering time and calyx tube width would have acted as one of the possible reproductive barriers in the six sister taxa pairs, and there are possibilities that the speciation triggered by trait differentiations may have also occurred in *Heterotropa*.

5. *Conclusion*

Qian & Ricklefs (2001) hypothesised that in East Asia, the climatic oscillation with topographic complexities could generate diversity of temperate plants through allopatric speciation. Although both biotic and abiotic factors have long been recognized as fundamental drivers of diversity, their relative contributions to the diversification had been rarely investigated especially by using specious plant groups (Funamoto, 2019). Our results implied that the repeated range fragmentations and contractions in the insular systems during the Pleistocene period formed the diversity anomaly, which basically supports the Qian & Ricklefs's hypothesis. Furthermore, the rates of floral trait evolution were correlated with the speciation rate, while most taxa are distributed allopatrically, at present. The sister-taxa analysis implied that speciation, triggered by reproductive trait differentiations without geographic isolation, could have occurred recently. Thus, the diversification appears to have been driven by multiple drivers, including geographic isolation and complemental floral trait evolution at different temporal

scales. Our study demonstrates the importance of multidimensional studies to understand the diversification process of temperate plants in the SJFR, where geographic isolation had been considered to play a dominant role in the diversification.

viii. Tables

Table 1. The proportions of taxa pairs showing geographic isolation and floral trait differentiation in the three major clades (mainland Japan, Ryukyu-Taiwan, and mainland China). The values within parentheses show the number of pairs showing overlap/differentiation and number of all pairs.

	Clade		
Attribute	Mainland Japan	Ryukyu-Taiwan	Mainland China
Geographic isolations	90.36% (704/780)	88.32% (311/351)	69.85% (95/136)
Flowering time differentiation	52.44% (409/780)	21.37% (75/351)	28.76% (44/153)
Calyx tube diameter differentiation	36.28% (283/780)	56.13% (197/351)	68.63% (105/153)

Table 2. Geographic overlap and morphological differences in the 24 sister-taxa pairs with more than 80% posterior support. For each sister-taxa pair, columns indicate the posterior probability that the two taxa are sister, proportion of range overlap, flowering time differentiation (month), calyx tube diameter differentiation (mm), estimated divergence time, and the clade name that includes two taxa.

Sister pair		Posterior probability	Geographical overlap	Flowering time differentiation	Calyx tube diameter differentiation	Estimated divergence time (Mya)	Clade name
A. fauriei	*A. titaensis*	100%	0	3†	4.5	1.07	Mainland Japan
A. blumei	*A. nipponicum*	100%	1.00	6†	3.0†	0.46	Mainland Japan
A. kinoshitae	*A. rigescens* var. *rigescens*	100%	1.00	2†	2.0†	1.63	Mainland Japan
A. fauriei var. *stoloniferum*	*A. kurosawae*	100%	0	6†	4.0†	1.27	Mainland Japan
A. ikegamii var. *fujimakii*	*A. megacalyx*	100%	1.00	0	3.5	1.07	Mainland Japan
A. muramatsui	*A. tamaense*	100%	0	0	0	0.84	Mainland Japan
A. satsumense K	*A. unzen*	100%	0	1	8.5†	1.01	Mainland Japan
A. curvistigma	*A. kiusiana* var. *tubulosum*	100%	0	2†	2.0	1.60	Mainland Japan
A. hexalobum var. *controversum*	*A. hexalobum* var. *perfectum*	100%	0	0	4.0†	2.23	Mainland Japan
A. kumagaeanum var. *satakeanum*	*A. lutchuense*	100%	0	0	2.5	0.83	Mainland Japan
A. crassum	*A. trigynum*	100%	0	0	3.0	2.39	Mainland Japan
A. ampulliflorum	*A. chatienshanianum*	100%	0	3	9.8†	0.86	Ryukyu-Taiwan
A. satsumense W	*A. macranthum*	84%	0.55	2	3.5	1.11	Ryukyu-Taiwan
A. gelasinum	*A. monodoriflorum*	83%	0.99	1	1.0†	1.15	Ryukyu-Taiwan
A. senkakuinsulare	*A. dissitum*	100%	0	2†	7.5†	1.01	Ryukyu-Taiwan
A. celsum	*A. gusk*	100%	0.90	2	6.5†	0.41	Ryukyu-Taiwan
A. crassusepalum	*A. taipingshanianum*	100%	0.17	0	1.3	1.27	Ryukyu-Taiwan

Table 2 continued

A. hypogynum	*A. tawushanianum*	100%	0	0	1.5	1.73	Ryukyu-Taiwan
A. crispulatum	*A. porphyronotum* var. *atrovirens*	100%	0.63	0	3.5	0.47	Mainland China
A. nobillisimum	*A. delavayi*	100%	-‡	1	2.5	0.29	Mainland China
A. splendens	*A. inflatum*	100%	0.33	1	10.0†	1.39	Mainland China
A. maximum	*A. nanchuanense*	80%	1.00	1	2.5	2.85	Mainland China
A. glabrum	*A. reticulatum*	100%	0	2†	7.0†	0.16	Mainland China
A. wulingense	*A. insigne*	100%	0.91	0	30†	0.52	Mainland China

†No overlap the between the pair ‡ We could not calculate the geographic overlap because there were no available records for *A. nobillisimum*.

ix. Figures

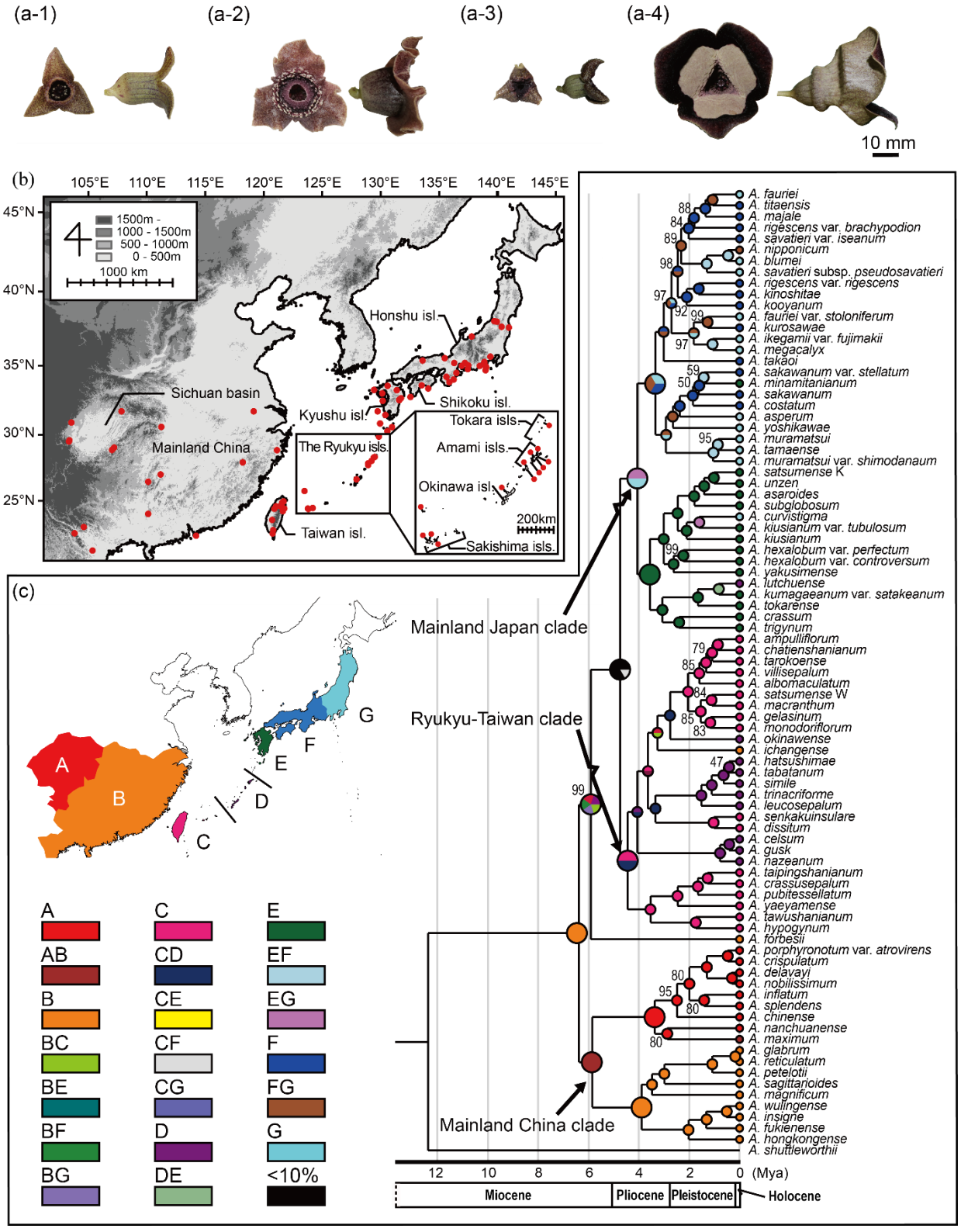
(a-1)
(a-2)
(a-3)
(a-4)
10 mm
(b)
105°E
110°E
115°E
120°E
125°E
130°E
135°E
140°E
145°E
45°N
40°N
35°N
30°N
25°N
1500m -
1000 - 1500m
500 - 1000m
0 - 500m
1000 km
Honshu isl.
Shikoku isl.
Kyushu isl.
Sichuan basin
Mainland China
The Ryukyu isls.
Tokara isls.
Amami isls.
Okinawa isl.
200km
Taiwan isl.
Sakishima isls.
(c)
A
B
C
D
E
F
G
A
AB
B
BC
BE
BF
BG
C
CD
CE
CF
CG
D
DE
E
EF
EG
F
FG
G
<10%
Mainland Japan clade
Ryukyu-Taiwan clade
Mainland China clade
A. fauriei
A. titaensis
A. majale
A. rigescens var. brachypodion
A. savatieri var. iseanum
A. nipponicum
A. blumei
A. savatieri subsp. pseudosavatieri
A. rigescens var. rigescens
A. kinoshitae
A. kooyanum
A. fauriei var. stoloniferum
A. kurosawae
A. ikegamii var. fujimakii
A. megacalyx
A. takaoi
A. sakawanum var. stellatum
A. minamitanianum
A. sakawanum
A. costatum
A. asperum
A. yoshikawae
A. muramatsui
A. tamaense
A. muramatsui var. shimodanaum
A. satsumense K
A. unzen
A. asaroides
A. subglobosum
A. curvistigma
A. kiusianum var. tubulosum
A. kiusianum
A. hexalobum var. perfectum
A. hexalobum var. controversum
A. yakusimense
A. lutchuense
A. kumagaeanum var. satakeanum
A. tokarense
A. crassum
A. trigynum
A. ampulliflorum
A. chatienshanianum
A. tarokoense
A. villisepalum
A. albomaculatum
A. satsumense W
A. macranthum
A. gelasinum
A. monodoriflorum
A. okinawense
A. ichangense
A. hatsushimae
A. tabatanum
A. simile
A. trinacriforme
A. leucosepalum
A. senkakuinsulare
A. dissitum
A. celsum
A. gusk
A. nazeanum
A. taipingshanianum
A. crassisepalum
A. pubitessellatum
A. yaeyamense
A. tawushanianum
A. hypogynum
A. forbesii
A. porphyronotum var. atrovirens
A. crispulatum
A. delavayi
A. nobilissimum
A. inflatum
A. splendens
A. chinense
A. nanchuanense
A. maximum
A. glabrum
A. reticulatum
A. petelotii
A. sagittarioides
A. magnificum
A. wulingense
A. insigne
A. fukienense
A. hongkongense
A. shuttleworthii
12
10
8
6
4
2
0
(Mya)
Miocene
Pliocene
Pleistocene
Holocene

Fig. 1. The diversification of *Heterotropa* in the Sino-Japanese Floristic region. (a) Photographs of the flowers of *Heterotropa* taxa (a-1; *Asarum takaoi*, a-2; *A. unzen*, a-3; *A. dissitum*, and a-4; *A. maximum*). (b) Map of the Sino-Japanese Floristic Region. Red circles indicate sampling points. (c) Time-calibrated molecular phylogenetic tree and the ancestral areas estimated from Bayesian analysis and statistical dispersal-vicariance analysis (S-DIVA). Posterior probabilities of < 100% are indicated above or below branches, and the branches without posterior probabilities are those with 100% support. The colours of pie charts reflect the estimated distribution areas according to the biogeographic delimitation as in map (A; Sichuan basin and surrounding mountains, B; other parts of mainland China, C; Taiwan and southern Ryukyu islands, D; central Ryukyu islands, E; northern Ryukyu islands and Kyushu island, F; southern part of mainland Japan including Shikoku island, and G; northern part of mainland Japan).

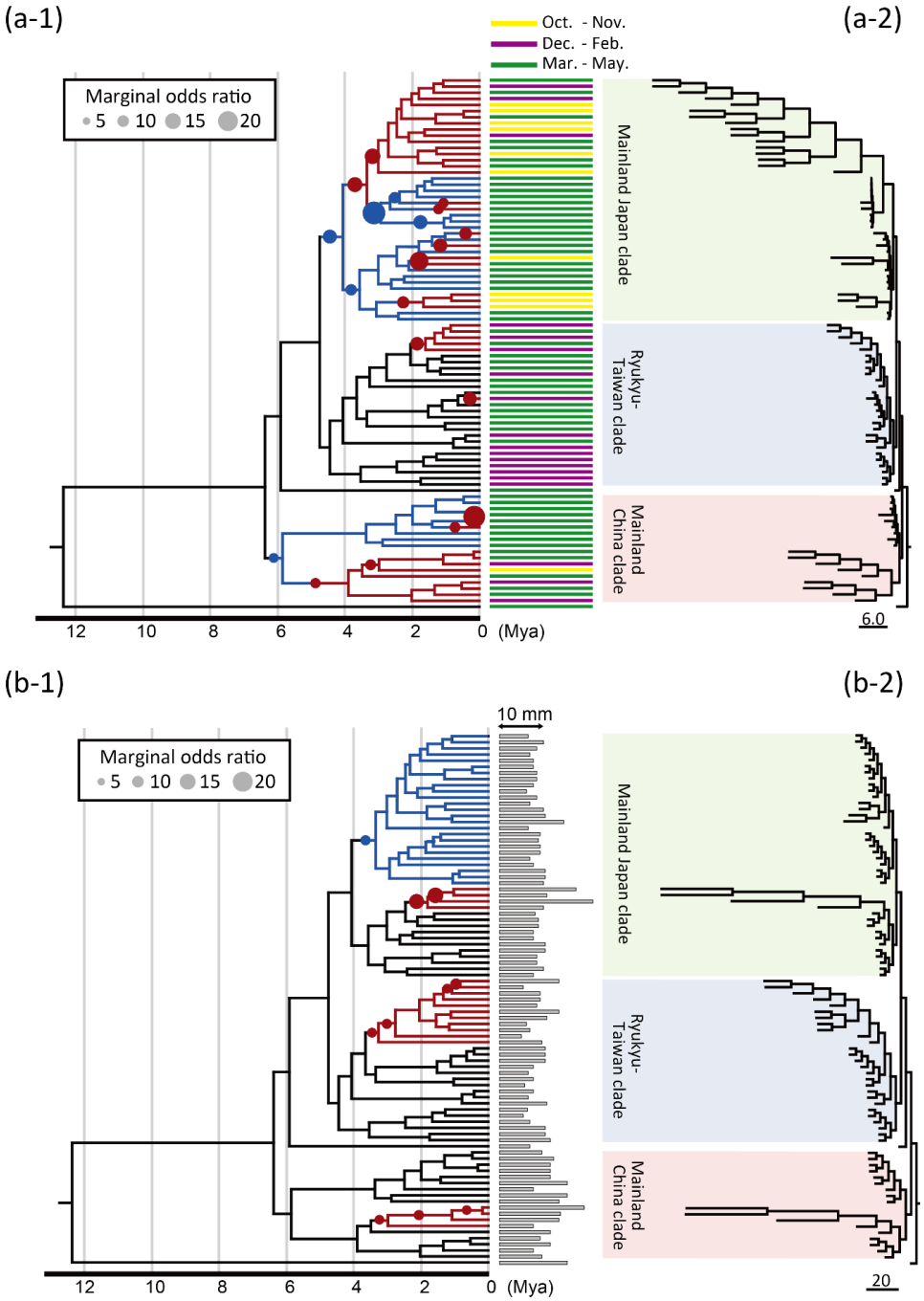
(a-1)
(a-2)
Oct. - Nov.
Dec. - Feb.
Mar. - May.
Marginal odds ratio
5 10 15 20
Mainland Japan clade
Ryukyu-Taiwan clade
Mainland China clade
12 10 8 6 4 2 0 (Mya)
6.0
(b-1)
(b-2)
10 mm
Marginal odds ratio
5 10 15 20
Mainland Japan clade
Ryukyu-Taiwan clade
Mainland China clade
12 10 8 6 4 2 0 (Mya)
20

Fig. 2. The results of BAMM analysis of flowering time (a), and calyx tube width (b). The circles on the left trees (a-1, b-1) show the locations of rate shifts with the size proportional to the marginal odds ratio of the shift. the colours of circles and branches are corresponded to the fluctuation of rates before and after the shift (red; rate increase and blue; rate decrease). The shifts with marginal odds below 5 are not shown. The branch lengths of right trees (a-2, b-2) are transformed to their marginal phenotypic evolution rates of each trait. The topologies of all trees are the same as in Figure 1. Colours and lengths of bars across the tips of the phylogenetic trees represent flowering time and mean calyx tube width (mm), respectively. Flowering times are classified conveniently into three types: autumn (flowering at September to November; purple), winter (flowering at December to February; yellow), and spring (flowering at March to June; green) in this figure, while BAMM analysis was conducted by using continuous variables of scaled flowering times (shown in Fig. S2).

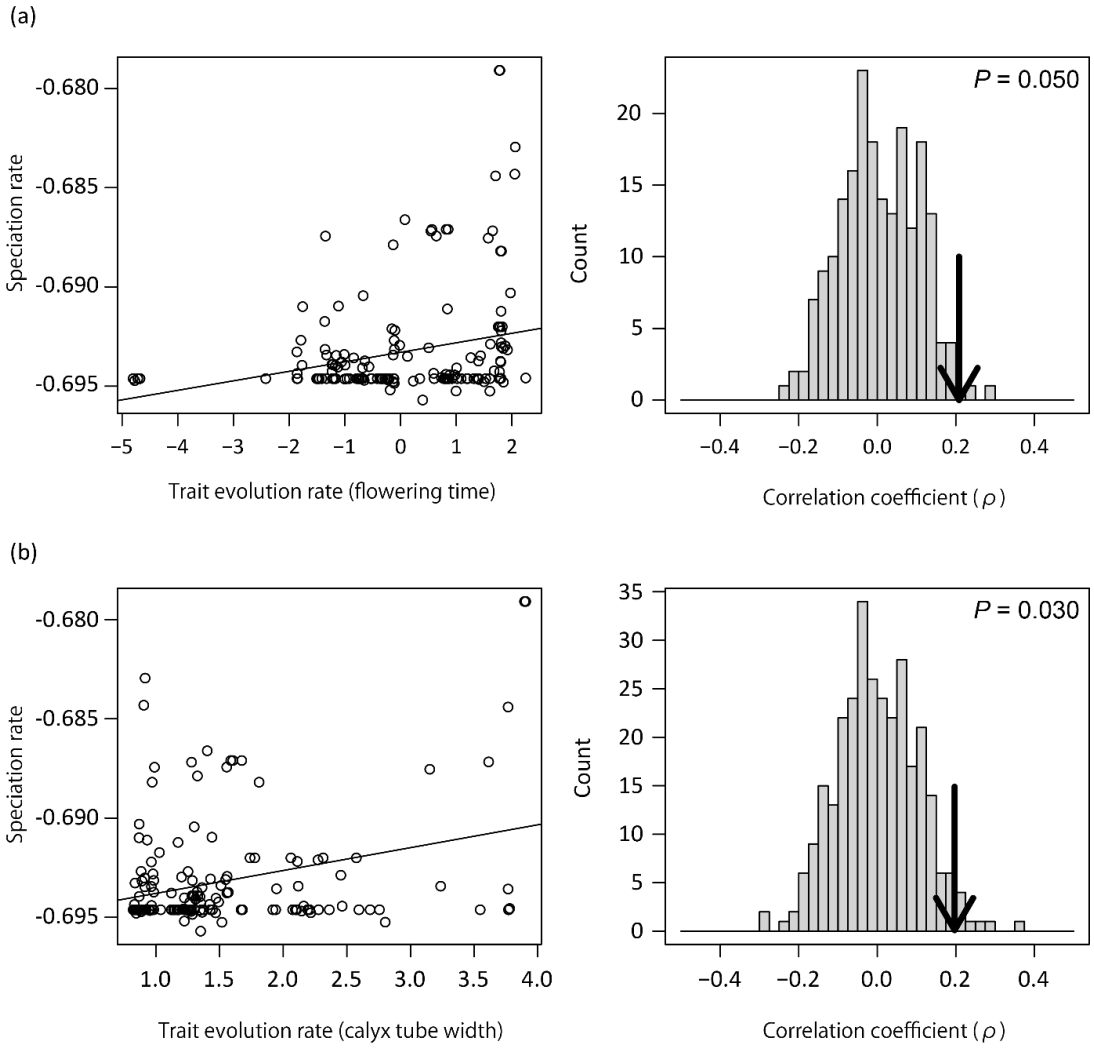

Fig. 3. Relationships between the speciation rate and each trait evolution rate; (a) flowering time, and (b) calyx tube width. Scatterplots (left column) show the relationships between log-transformed rates of speciation and floral trait evolution estimated from BAMM. Right column shows histograms of Spearman's rank correlation coefficients (ρ) calculated from 200 simulated datasets. Arrows represent the ρ value calculated from observed trait evolution rates and speciation rate.

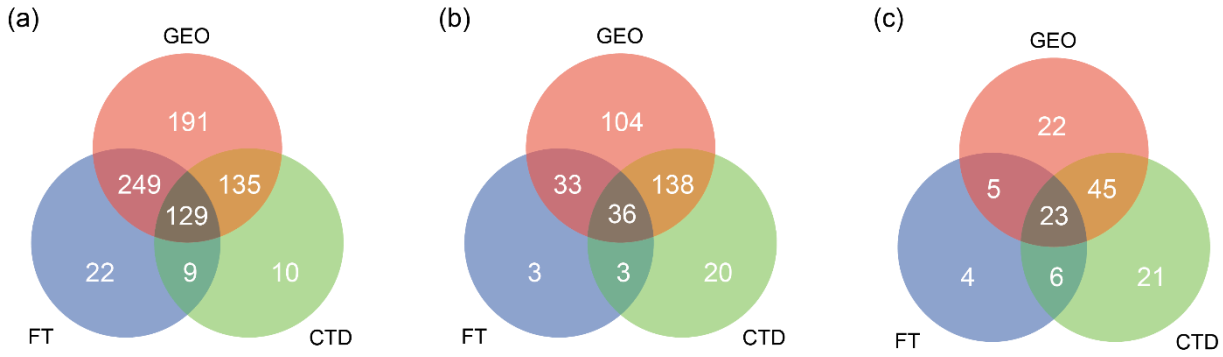

Fig. 4. Venn diagrams showing the number of taxa pairs with non-overlap of distribution range (GEO; red), and differentiation in flowering time (FT; blue) and in calyx tube diameter (CTD; green) within mainland Japan clade (a), Ryukyu-Taiwan clade (b), and mainland China clade (c).

x. Data accessibility statement

The obtained reads for chloroplast genome construction and ddRAD-seq analysis are available in NCBI (GenBank BioProject no. PRJDB9302 and PRJDB8943) The alignment sequences, morphological data, and distribution records were deposited in the Dryad® digital repository under doi: 10.5061/dryad.xwdbrv1b4.

xi. References

Anacker, B. L., & Strauss, S. Y. (2014). The geography and ecology of plant speciation: range overlap and niche divergence in sister species. *Proceedings of the Royal Society B-Biological Sciences, 281*(1778). doi:10.1098/rspb.2013.2980

Aoki, K., Tamaki, I., Nakao, K., Ueno, S., Kamijo, T., Setoguchi, H., . . . Tsumura, Y. (2019). Approximate Bayesian computation analysis of EST-associated microsatellites indicates that the broadleaved evergreen tree *Castanopsis sieboldii* survived the Last Glacial Maximum in multiple refugia in Japan. *Heredity, 122*(3), 326.

Armbruster, W. S. (2014). Floral specialization and angiosperm diversity: phenotypic divergence, fitness trade-offs and realized pollination accuracy. *Aob Plants, 6*. doi:10.1093/aobpla/plu003

Boucher, F. C., Zimmermann, N. E., & Conti, E. (2016). Allopatric speciation with little niche divergence is common among alpine Primulaceae. *Journal of Biogeography, 43*(3), 591-602. doi:10.1111/jbi.12652

Cooney, C. R., & Thomas, G. H. (2021). Heterogeneous relationships between rates of speciation and body size evolution across vertebrate clades. *Nature Ecology & Evolution, 5*(1). doi:10.1038/s41559-020-01321-y

Devaux, C., & Lande, R. (2008). Incipient allochronic speciation due to non-selective assortative mating by flowering time, mutation and genetic drift. *Proceedings of the Royal Society B-Biological Sciences, 275*(1652), 2723-2732. doi:10.1098/rspb.2008.0882

Fenster, C. B., Armbruster, W. S., Wilson, P., Dudash, M. R., & Thomson, J. D. (2004). Pollination syndromes and floral specialization. *Annual Review of Ecology Evolution and Systematics, 35*, 375-403. doi:10.1146/annurev.ecolsys.34.011802.132347

Funamoto, D. (2019). Plant-pollinator interactions in east Asia: A review. *Journal of Pollination Ecology, 25*(6), 46-68.

Gao, Y. D., Zhang, Y., Gao, X. F., & Zhu, Z. M. (2015). Pleistocene glaciations, demographic expansion and subsequent isolation promoted morphological heterogeneity: A phylogeographic study of the alpine *Rosa sericea* complex (Rosaceae). *Scientific Reports, 5*. doi:10.1038/srep11698

Givnish, T. J., Spalink, D., Ames, M., Lyon, S. P., Hunter, S. J., Zuluaga, A., . . . Cameron, K. M. (2015). Orchid phylogenomics and multiple drivers of their extraordinary diversification. *Proceedings of the Royal Society B-Biological Sciences, 282*(1814), 171-180. doi:10.1098/rspb.2015.1553

Haq, B. U., Hardenbol, J., & Vail, P. R. (1987). Chronology of fluctuating sea levels since the Triassic. *Science, 235*(4793), 1156-1167.

Harmon, L. J., Weir, J. T., Brock, C. D., Glor, R. E., & Challenger, W. (2008). GEIGER: investigating evolutionary radiations. *Bioinformatics, 24*(1), 129-131. doi:10.1093/bioinformatics/btm538

Harrison, S. P., Yu, G., Takahara, H., & Prentice, I. C. (2001). Palaeovegetation - Diversity of temperate plants in east Asia. *Nature, 413*(6852), 129-130. doi:10.1038/35093166

Hiura, I. (1978). The histories traced by the butterfly (in Japanese). In. Tokyo: Aoki shobou.

Ho, L. S. T., Ane, C., Lachlan, R., Tarpinian, K., Feldman, R., Yu, Q., . . . Ho, M. L. S. T. (2016). Package 'phylolm'. *See http://cran. r-project. org/web/packages/phylolm/index. html (accessed February 2018)*.

Jaramillo, M. A., & Manos, P. S. (2001). Phylogeny and patterns of floral diversity in the genus *Piper* (Piperaceae). *American Journal of Botany, 88*(4), 706-716. doi:10.2307/2657072

Kakishima, S., & Okuyama, Y. (2018). Floral scent profiles and flower visitors in species of *Asarum* Series Sakawanum (Aristolochiaceae). *J Bulletin of the National Museum of Nature and Science. Series B, Botany, 44*(1), 41-51.

Kimura, M. (1996). Quaternary paleogeography of the Ryukyu Arc. *Journal of Geography Tokyo, 105*, 259-285.

Kinoshita, S. (1973). Obituary of the Late Mr. Y. Kato. *Journal of Geobotany, 26*(4), 109-111.

Kishi, K., & Irizawa, S. (2008). *Wild ginger, Asarum (in Japanese)*. Tochigi, Japan: Tochinoha-shobo.

Lagomarsino, L. P., Condamine, F. L., Antonelli, A., Mulch, A., & Davis, C. C. (2016). The abiotic and biotic drivers of rapid diversification in Andean bellflowers (Campanulaceae). *New Phytologist, 210*(4), 1430-1442. doi:10.1111/nph.13920

Lande, R. (2000). Quantitative genetics and phenotypic evolution. In R. C. Lewontin & K. V. Krimpas (Eds.), *Evolutionary Genetics: From Molecules to Morphology (Vol. 1)* (pp. 335-350). Cambridge, UK: Cambridge University Press.

Landrein, S., Buerki, S., Wang, H. F., & Clarkson, J. J. (2017). Untangling the reticulate history of species complexes and horticultural breeds in Abelia (Caprifoliaceae). *Annals of Botany, 120*(2), 257-269. doi:10.1093/aob/mcw279

Lu, C.-T., Chiou, W.-L., Liu, S.-C., & Wang, J.-C. (2010). *Asarum satsumense* F. Maekawa (Aristolochiaceae), a newly recorded species in Taiwan. *Taiwania, 55*(4), 396-401.

Maekawa, F. (1983). *Heterotropa kiusiana*. In R. Ishii & Y. Inoue (Eds.), *Encyclopedia of horticulture* (Vol. 5). Tokyo, Japan: Seibundo-Shinkosha.

Matsuda, J., Maeda, Y., Nagasawa, J., & Setoguchi, H. (2017). Tight species cohesion among sympatric insular wild gingers (*Asarum* spp. Aristolochiaceae) on continental islands: Highly differentiated floral characteristics versus undifferentiated

genotypes. *Plos One, 12*(3). doi:10.1371/journal.pone.0173489

Mitsui, Y., Chen, S. T., Zhou, Z. K., Peng, C. I., Deng, Y. F., & Setoguchi, H. (2008). Phylogeny and biogeography of the genus *Ainsliaea* (Asteraceae) in the Sino-Japanese region based on nuclear rDNA and plastid DNA sequence data. *Annals of Botany, 101*(1), 111-124. doi:10.1093/aob/mcm267

Mitsui, Y., Nomura, N., Isagi, Y., Tobe, H., & Setoguchi, H. (2011). Ecological barriers to gene flow between riparian and forest species of *Ainsliaea* (Asteraceae). *Evolution, 65*(2), 335-349. doi:10.1111/j.1558-5646.2010.01129.x

Nakamura, K., Suwa, R., Denda, T., & Yokota, M. (2009). Geohistorical and current environmental influences on floristic differentiation in the Ryukyu Archipelago, Japan. *Journal of Biogeography, 36*(5), 919-928. doi:10.1111/j.1365-2699.2008.02057.x

Okaura, T., Quang, N. D., Ubukata, M., & Harada, K. (2007). Phylogeographic structure and late Quaternary population history of the Japanese oak Quercus mongolica var. crispula and related species revealed by chloroplast DNA variation. *Genes & Genetic Systems, 82*(6), 465-477. doi:10.1266/ggs.82.465

Okuyama, Y., Goto, N., Nagano, A. J., Yasugi, M., Kokubugata, G., Kudoh, H., . . . Sugawara, T. (2020). Radiation history of Asian *Asarum* (sect. *Heterotropa*, Aristolochiaceae) resolved using a phylogenomic approach based on double-digested RAD-seq data. *Annals of Botany, 126*(2), 245-260. doi:10.1093/aob/mcaa072

Pebesma, E. (2018). Simple features for R: standardized support for spatial vector data. *The R Journal, 10*(1), 439-446.

Petit, R. J., Duminil, J., Fineschi, S., Hampe, A., Salvini, D., & Vendramin, G. G. (2005). Comparative organization of chloroplast, mitochondrial and nuclear diversity in plant populations. *Molecular Ecology, 14*(3), 689-701. doi:10.1111/j.1365-294X.2004.02410.x

Qi, X. S., Chen, C., Comes, H. P., Sakaguchi, S., Liu, Y. H., Tanaka, N., . . . Qiu, Y. X. (2012). Molecular data and ecological niche modelling reveal a highly dynamic evolutionary history of the East Asian Tertiary relict *Cercidiphyllum* (Cercidiphyllaceae). *New Phytologist, 196*(2), 617-630. doi:10.1111/j.1469-8137.2012.04242.x

Qian, H., & Ricklefs, R. E. (2000). Large-scale processes and the Asian bias in species diversity of temperate plants. *Nature, 407*(6801), 180-182.

Qiu, Y. X., Fu, C. X., & Comes, H. P. (2011). Plant molecular phylogeography in China and adjacent regions: Tracing the genetic imprints of Quaternary climate and environmental change in the world's most diverse temperate flora. *Molecular Phylogenetics and Evolution, 59*(1), 225-244. doi:10.1016/j.ympev.2011.01.012

R Core Team. (2013). R: A language and environment for statistical computing.

Rabosky, D. L. (2014). Automatic Detection of Key Innovations, Rate Shifts, and Diversity-Dependence on Phylogenetic Trees. *Plos One, 9*(2). doi:10.1371/journal.pone.0089543

Rabosky, D. L., Grundler, M., Anderson, C., Title, P., Shi, J. J., Brown, J. W., . . . Larson, J. G. (2014). BAMMtools: an R package for the analysis of evolutionary dynamics on phylogenetic trees. *Methods in Ecology and Evolution, 5*(7), 701-707. doi:10.1111/2041-210x.12199

Revell, L. J. (2012). phytools: an R package for phylogenetic comparative biology (and other things). *Methods in Ecology and Evolution, 3*(2), 217-223. doi:10.1111/j.2041-210X.2011.00169.x

Rundle, H. D., & Nosil, P. (2005). Ecological speciation. *Ecology Letters, 8*(3), 336-352. doi:10.1111/j.1461-0248.2004.00715.x

Shi, J. J., & Rabosky, D. L. (2015). Speciation dynamics during the global radiation of extant bats. *Evolution, 69*(6), 1528-1545. doi:10.1111/evo.12681

Sinn, B. T., Kelly, L. M., & Freudenstein, J. V. (2015). Putative floral brood-site mimicry, loss of autonomous selfing, and reduced vegetative growth are significantly correlated with increased diversification in Asarum (Aristolochiaceae). *Molecular Phylogenetics and Evolution, 89*, 194-204. doi:10.1016/j.ympev.2015.04.019

Sugawara, T. (1987). Taxonomic studies of *Asarum* sensu lato III. comparative floral anatomy. *Botanical Magazine-Tokyo, 100*(1060), 335-348. doi:10.1007/bf02488853

Sugawara, T. (1988). Floral biology of *Heterotropa tamaensis* (Aristolochiaceae) in Japan. *Plant Species Biology, 3*(1), 7-12.

Sugawara, T. (2006). Aristorochiaceae. In K. Iwatsuki, D. E. Boufford, & H. Ohba (Eds.), *Flora of Japan* (Vol. 2a). Tokyo: Kodansha.

Sugawara, T., & Ogisu, M. (1992). Karyomorphology of 11 species of *Asarum* (Aristolochiaceae) from Taiwan and mainland China. *Acta Phytotaxonomica et Geobotanica, 43*(2), 89-96.

Takahashi, D., & Setoguchi, H. (2018). Molecular phylogeny and taxonomic implications of *Asarum* (Aristolochiaceae) based on ITS and matK sequences. *Plant Species Biology, 33*(1), 28-41. doi:10.1111/1442-1984.12189

Ujiie, H. (1990). Geological history of the Ryukyu Island arc. *Nature of Okinawa; geomorphology and geology. Hirugisha, Naha*, 251-255.

Wang, Y. H., Jiang, W. M., Comes, H. P., Hu, F. S., Qiu, Y. X., & Fu, C. X. (2015). Molecular phylogeography and ecological niche modelling of a widespread herbaceous climber, *Tetrastigma hemsleyanum* (Vitaceae): insights into Plio–Pleistocene range dynamics of evergreen forest in subtropical China. *New Phytologist, 206*(2), 852-867.

Weber, M. G., & Strauss, S. Y. (2016). Coexistence in Close Relatives: Beyond Competition and Reproductive Isolation in Sister Taxa. *Annual Review of Ecology, Evolution, and Systematics, Vol 47, 47*, 359-381. doi:10.1146/annurev-ecolsys-112414-054048

Wu, Z., & Wu, S. (1996). *A proposal for a new floristic kingdom (realm)-the E. Asiatic kingdom, its delineation and characteristics*. Beijing, China/Berlin, Heidelberg, Germany: Beijing: China Higher Education Press/Springer-Verlag.

Yang, L. Q., Hu, H. Y., Xie, C., Lai, S. P., Yang, M., He, X. J., & Zhou, S. D. (2017). Molecular phylogeny, biogeography and ecological niche modelling of *Cardiocrinum* (Liliaceae): insights into the evolutionary history of endemic genera distributed across the Sino-Japanese floristic region. *Annals of Botany, 119*(1), 59-72. doi:10.1093/aob/mcw210

Yoichi, W., Jin, X. F., Peng, C. I., Tamaki, I., & Tomaru, N. (2017). Contrasting diversification history between insular and continental species of three-leaved azaleas (Rhododendron sect. Brachycalyx) in East Asia. *Journal of Biogeography, 44*(5), 1065-1076. doi:10.1111/jbi.12924

Yu, Y., Harris, A. J., & He, X. J. (2010). S-DIVA (Statistical Dispersal-Vicariance Analysis): A tool for inferring biogeographic histories. *Molecular Phylogenetics and Evolution, 56*(2), 848-850. doi:10.1016/j.ympev.2010.04.011

xii. Biosketch

Daiki Takahashi is a PhD student in Kyoto University; his research interests include biogeographical factor and ecological processes shaping floristic diversity in plants of East Asia.

Editor: Alain Vanderpoorten

Author contributions: D. T., S. S., Y. Q., Y. I., and H. S. conceptualised and designed the study. Sample collection was performed by D. T., S. S., Y. F., Y. Q., Y. I., P. L., R. L., C. L., S. C., Y. L., Y. C., and H. S. The molecular experiments were conducted by D. T., S. S., L. K., and A. N., Data were generated, analysed, and visualised by D. T. and S. S. Manuscript writing was led by D. T., with contributions from all authors.

Appendix 1

Chloroplast genome construction and divergence time estimation

To obtain the chloroplast genomes, we sequenced four *Heterotropa* species (*Asarum satsumense* K, *A. macranthum*, *A. wulingense*, and *A. forbesii*) and one *Hexastylis* species (*Asarum shuttleworthii*). We used three sequencing methods.

To *A. macranthum* and *A. wulingense*, we used the chloroplast enrichment method following Sakaguchi *et al.* (2017). To construct barcoded DNA fragment libraries, the Ion Xpress Plus Fragment library Kit (Thermo Fisher Scientific, Waltham, Massachusetts, USA) was used to process the purified DNA of *A. macranthum* and *A. wulingense*. The barcoded libraries were mixed with Ion Sphere Particle for emulsion PCR using Ion One Touch 2 system (Thermo Fisher Scientific) with Ion PGM Hi-Q OT2 Kit (Thermo Fisher Scientific). From the product of emulsion PCR, the positive particles with amplified DNA were isolated and purified by Ion OneTouch ES (Thermo Fisher Scientific) and loaded onto an Ion 318 chip (Thermo Fisher Scientific). Sequencing was performed using an Ion PGM sequencer (Thermo Fisher Scientific). Extracted DNA from *A. satsumense* K and *A. shuttleworthii* were fragmented using the Takara DNA Fragmentation Kit (Takara Bio, Ohtsu, Shiga, Japan). The library preparation was conducted using the SMARTer ThruPLEX DNA-Seq Kit (Takara Bio, USA). Barcoded libraries were sequenced with paired-end 150 bp reads on Illumina Hiseq-X (Illumina, San Diego, California, USA; sequencing was performed by Macrogen Japan, Kyoto, Japan). To *A. forbesii*, NEBNext® DNA Library Prep Kit (New England BioLabs, Ipswich, MA, USA) was used to prepare library. Nova-seq 6000 (Illumina) was used to sequence the prepared library. Library preparation and sequencing were performed by Chemical Dojin (Kumamoto, Japan).

All obtained reads were trimmed using Trimomomatic v. 0.32 software (Bolger, Lohse, & Usadel, 2014) using the following commands: HEADCRAP:10, LEADING:20, TRAILING:20, SLIDINGWINDOW:4:20, AVGQUAL:20, and MINLEN:50. Because the amount of obtained reads of *A. forbesii* was too large (> 80 Gb), we reduced the data to 500,000 reads (approximately 7.5 Gb). The cleaned reads were mapped using MITObim v.1.8 (Hahn, Bachmann, & Chevreux, 2013) to the chloroplast genome of *A. costatum* (AP018513; Daiki Takahashi, Sakaguchi, Isagi, & Setoguchi, 2018) with minimum depth 4X. The obtained reads and chloroplast genomes were deposited in DDBJ (BioProject ID, PRJDB9302, Table S2).

To construct chloroplast genome phylogeny and estimate divergence time, in addition to newly obtained five sequences, we used the chloroplast genome sequences of

ten Magnoliid species, including one *Heterotropa* species (*A. costatum*), and two Chloranthales species. The species information is shown in Table S3. As our data set included highly divergent species, to construct the chloroplast phylogeny, we used only CDS regions shared by more than 17 species out of 18 species. The CDS regions of chloroplast genomes and assemblies were identified using GeSeq with protein search identity value 85 (Tillich et al., 2017). Sequence data were manually edited and aligned using BioEdit v.7.0.5.3 (Hall, 1999). In total, 59 regions (26,786 bp) were used for the phylogenetic analysis. The phylogenetic tree construction and estimation of divergence time was conducted by using BEAST v.10.0.4 (Drummond & Rambaut, 2007) applying the GTR+I+G model inferred by JmodelTest v.1.4.7 (Posada, 2008). To estimate the divergence time of the crown age of the *Heterotropa* clade, the crown of Magnoliids was constrained using a uniform distribution with a lower bound of 169 Mya and upper bound of 180 Mya according to the study of angiosperm phylogeny using fossil calibrations (Zeng et al., 2014). The Markov Chain Monte Carlo method was performed using four independent runs with four chains of 50,000,000 generations each, saving one tree every 1000 generations. The first 10,000,000 generations were discarded as burn-in, as evaluated by TRACER v.1.5 (Rambaut & Drummond, 2013). The obtained tree was displayed using FigTree v.1.4 (Rambaut, 2009).

Double-digest restriction-associated DNA sequencing (ddRAD-seq)

Genomic DNA was extracted from silica-dried leaf tissues using the CTAB method (Doyle & Doyle, 1987). For all collected samples, a double-digest restriction-associated DNA library was prepared using Peterson's protocol with slight modifications (Peterson, Weber, Kay, Fisher, & Hoekstra, 2012). Genomic DNA was digested with BglII and EcoRI, ligated with Y-shaped adaptors, amplified by PCR with KAPA HiFi HS ReadyMix (KAPA BIOSYSTEMS) and size-selected with the E-Gel size select (Life Technologies, CA, USA). Approximately 350 bp of library fragments were retrieved. Further details of the library preparation method were described in a previous study (Sakaguchi et al., 2015). Sequencing was performed with paired-read 101bp + 100bp mode of HiSeq2500 (Illumina, CA, USA).

Data processing and phylogenetic analysis of ddRAD-seq data

The ddRAD-seq reads generated by Illumina sequencing were deposited in GenBank (BioProject ID: PRJDB8943). The raw reads were trimmed by Trimomomatic v. 0.32 software (Bolger et al., 2014) with the following settings: HEADCRAP:10, LEADING:30, TRAILING:30, SLIDINGWINDOW:4:30, AVGQUAL:30, and

MINLEN:50. The program ipyrad (http://github.com/dereneaton/ipyrad) was used to process the ddRAD-seq reads and detect SNPs. The parameters that influenced the assembly were set as follows: the minimum depth coverage for base calling at each locus was set at 6 and the similarity threshold for clustering reads within/across samples was set at 0.85. Potential paralogous loci were filtered out based on the number of samples with shared heterozygous sites (more than 15 sites). We explored a range of thresholds for the minimum genotyped samples (30, 51, and 70 samples; equivalent to 50%, 75%, and 90% of samples were genotyped, respectively). All three data sets were examined in the phylogenetic analysis, and we selected the 50% genotyped data set as the primary data set for all other analyses (see Results section).

To construct a phylogenetic tree of ddRAD-seq data and estimate divergence times within the *Heterotropa* clade, we used Bayesian inference (BI) in BEAST v. 1.10.4 (Drummond & Rambaut, 2007). We calibrated the crown age of the *Heterotropa* clade using a uniform distribution with lower limit of 4.77 Mya and upper limit of 14.54 Mya following the results of the chloroplast genome phylogenetic analysis (see Results section). The Markov Chain Monte Carlo (MCMC) method was performed using two simultaneous independent runs with four chains each (one cold and three heated), saving one tree every 1000 generations for a total 30,000,000 generations with 10% burn-in for each run. The convergence of the chains was checked using the program Tracer v. 1.5 (Rambaut & Drummond, 2013).

Collection of the floral trait data

In this study, we focused on two floral traits of *Heterotropa*; flowering time, which we defined as a month when the taxon starts flowering, and calyx tube width, defined as a median value between maximum and minimum calyx tube diameters. The trait values were obtained from literatures (Huang, Kelly, & Gilbert, 2003; C. T. Lu & Wang, 2009; Sugawara, 2006). Because these literatures refer to the description paper of each taxon, and *Heterotropa* taxa show relatively small intraspecific variation in calyx tube diameter (C. T. Lu & Wang, 2009, Sugawara 2006, Takahashi et al., in prep), we considered that the median values would represent the trait in nature.

Ancestral state reconstruction

In order to confirm the results of BAMM analysis for flowering time evolution, we also carried out ancestral state reconstruction analysis using single-rate model in “phytools” package (Revell, 2012). The flowering time of *Heterotropa* was treated as a discreate character, and we conducted the analysis for flowering time with eight states

(corresponded with the month) and with three states (autumn; flowering at October to November, winter; flowering at December to February, and spring; flowering at March to May), respectively.

Reference lists

Bolger, A. M., Lohse, M., & Usadel, B. (2014). Trimmomatic: a flexible trimmer for Illumina sequence data. *Bioinformatics, 30*(15), 2114-2120. doi:10.1093/bioinformatics/btu170

Doyle, J., & Doyle, J. (1987). Genomic plant DNA preparation from fresh tissue-CTAB method. *Phytochem Bull, 19*(11), 11-15.

Drummond, A. J., & Rambaut, A. (2007). BEAST: Bayesian evolutionary analysis by sampling trees. *Bmc Evolutionary Biology, 7*, 8. doi:10.1186/1471-2148-7-214

Hahn, C., Bachmann, L., & Chevreux, B. (2013). Reconstructing mitochondrial genomes directly from genomic next-generation sequencing reads-a baiting and iterative mapping approach. *Nucleic Acids Research, 41*(13). doi:10.1093/nar/gkt371

Hall, T. A. (1999). *BioEdit: a user-friendly biological sequence alignment editor and analysis program for Windows 95/98/NT.* Paper presented at the Nucleic acids symposium series.

Huang, S., Kelly, L. M., & Gilbert, M. G. (2003). *Aristolochiaceae* (Vol. 5): Science Press.

Lu, C. T., & Wang, J. C. (2009). Three new species of *Asarum* (section *Heterotropa*) from Taiwan. *Botanical Studies, 50*(2), 229-240.

Peterson, B. K., Weber, J. N., Kay, E. H., Fisher, H. S., & Hoekstra, H. E. (2012). Double Digest RADseq: An Inexpensive Method for De Novo SNP Discovery and Genotyping in Model and Non-Model Species. *Plos One, 7*(5). doi:10.1371/journal.pone.0037135

Posada, D. (2008). jModelTest: Phylogenetic model averaging. *Molecular Biology and Evolution, 25*(7), 1253-1256. doi:10.1093/molbev/msn083

Rambaut, A. (2009). FigTree v1. 4: Tree figure drawing tool. In.

Rambaut, A., & Drummond, A. J. (2013). Tracer v1. 5 Available from http://beast. bio. ed. ac. uk/Tracer. In: Accessed.

Revell, L. J. (2012). phytools: an R package for phylogenetic comparative biology (and other things). *Methods in Ecology and Evolution, 3*(2), 217-223. doi:10.1111/j.2041-210X.2011.00169.x

Sakaguchi, S., Sugino, T., Tsumura, Y., Ito, M., Crisp, M. D., Bowman, D., . . . Isagi, Y. (2015). High-throughput linkage mapping of Australian white cypress pine (*Callitris glaucophylla*) and map transferability to related species. *Tree Genetics & Genomes, 11*(6). doi:10.1007/s11295-015-0944-0

Sakaguchi, S., Ueno, S., Tsumura, Y., Setoguchi, H., Ito, M., Hattori, C., . . . Isagi, Y. (2017). Application of simplified method of chloroplast enrichment to small amounts of tissues for chloroplast genome sequencing. *Applications in Plant Sciences, 5*(5). doi:10.3732/apps.1700002

Sugawara, T. (2006). Aristorochiaceae. In K. Iwatsuki, D. E. Boufford, & H. Ohba (Eds.), *Flora of Japan* (Vol. 2a). Tokyo: Kodansha.

Takahashi, D., Sakaguchi, S., Isagi, Y., & Setoguchi, H. (2018). Comparative chloroplast genomics of series *Sakawanum* in genus *Asarum* (Aristolochiaceae) to develop single nucleotide polymorphisms (SNPs) and simple sequence repeat (SSR) markers. *Journal of Forest Research, 23*(6), 387-392.

Tillich, M., Lehwark, P., Pellizzer, T., Ulbricht-Jones, E. S., Fischer, A., Bock, R., & Greiner, S. (2017). GeSeq - versatile and accurate annotation of organelle genomes. *Nucleic Acids Research, 45*(W1), W6-W11. doi:10.1093/nar/gkx391

Zeng, L. P., Zhang, Q., Sun, R. R., Kong, H. Z., Zhang, N., & Ma, H. (2014). Resolution of deep angiosperm phylogeny using conserved nuclear genes and estimates of early divergence times. *Nature Communications, 5*. doi:10.1038/ncomms5956

Supplementary Figures and Tables

Fig. S1. Part of the floral diversity of *Heterotropa* taxa. The font and the side views of the flowers of *Asarum takaoi* (a), *A. savatieri* var. *iseanum* (b), *A. nipponicum* (c), *A. hexalobum* var. *perfectum* (d), *A. rigescens* (e), *A. costatum* (f), *A. trigynum* (g), *A. sakawanum* var. *stellatum* (h), *A. satsumense* K (i), *A. dissitum* (j), *A. pellucidum* (k), *A. gusk* (l), *A. senkakuinsulare* (m), *A. yaeyamense* (n), *A. tokarense* (o), *A. villisepalum* (p), *A. hypogynum* (q), *A. chatienshanianum* (r), *A. macranthum* (s), *A. forbesii* (t), *A. insigne* (u), *A. delavayi* (v), *A. petelotii* (w), *A. inflatum* (x), and *A. maximum* (y). The taxa were ordered according to their distributions: mainland Japan (a-h), the Ryukyu Islands (i-o), Taiwan (p-s), and mainland China (t-y). The colours of the alphabet indicate the flowering time of the taxa (red; autumn, blue; winter, and green; spring).

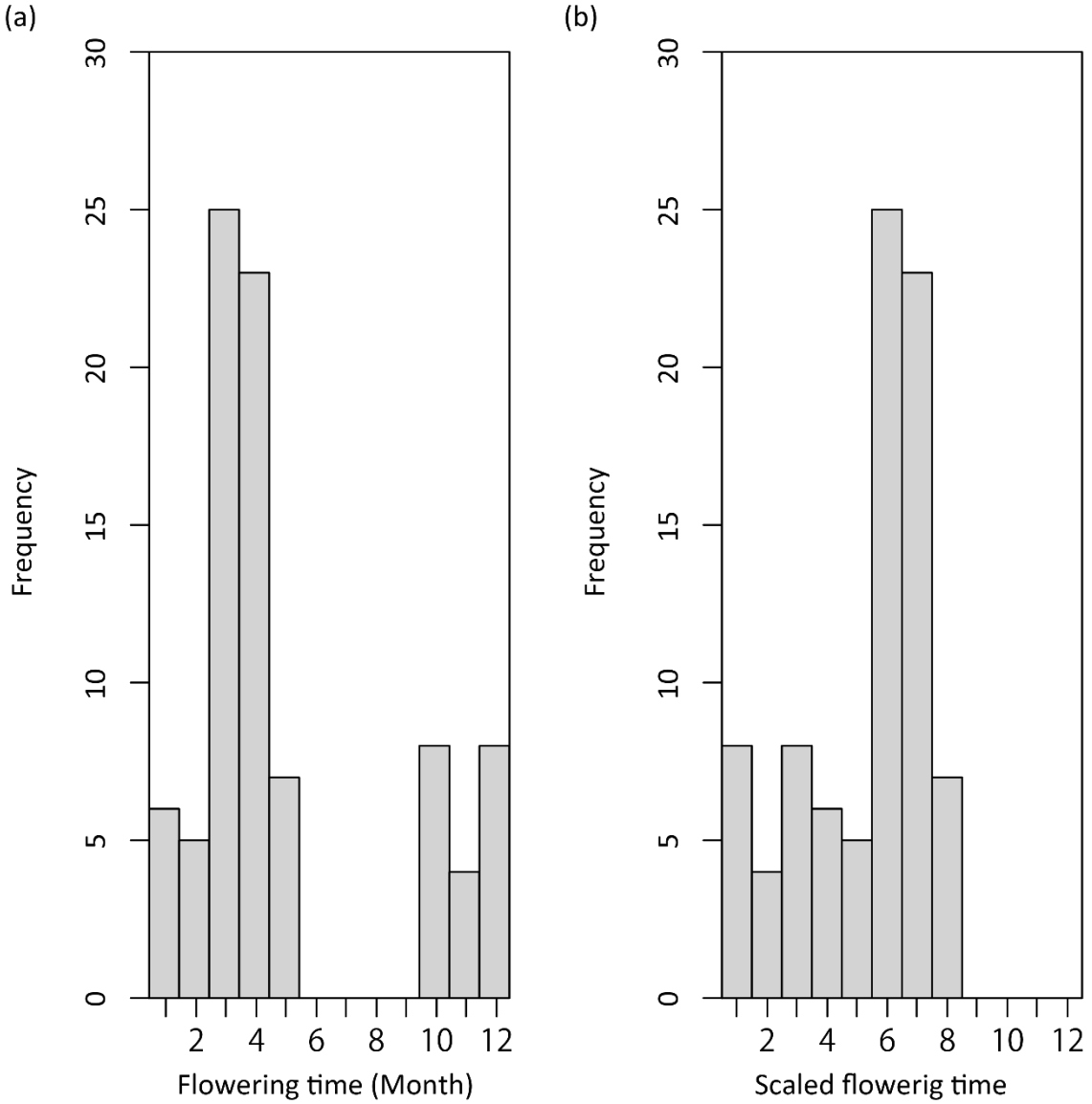

Fig. S2. Histograms of Flowering time of *Heterotropa* taxa; raw data (a), and scaled data used in the BAMM analysis (b).

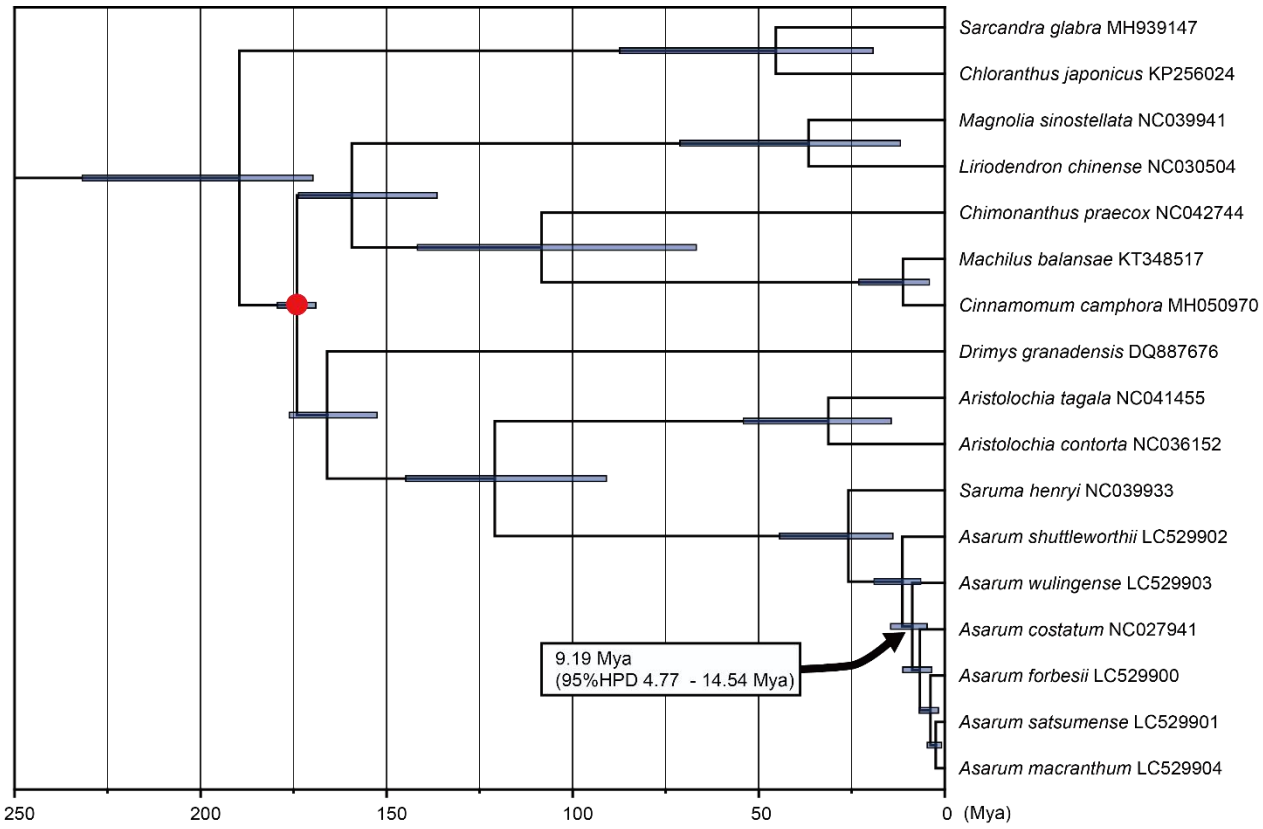

Fig. S3. Phylogenetic tree based on 59 CDS regions (26,786bp) of the chloroplast genomes of the Magnoliids and Chloranthales species. The red circle indicates the calibration point (169 – 180 Mya) followed by Zeng et al. (2014). The bars indicated 95% highest posterior density (HPD) intervals of estimated divergence times of nodes. The posterior probabilities of all the blanches were > 0.999.

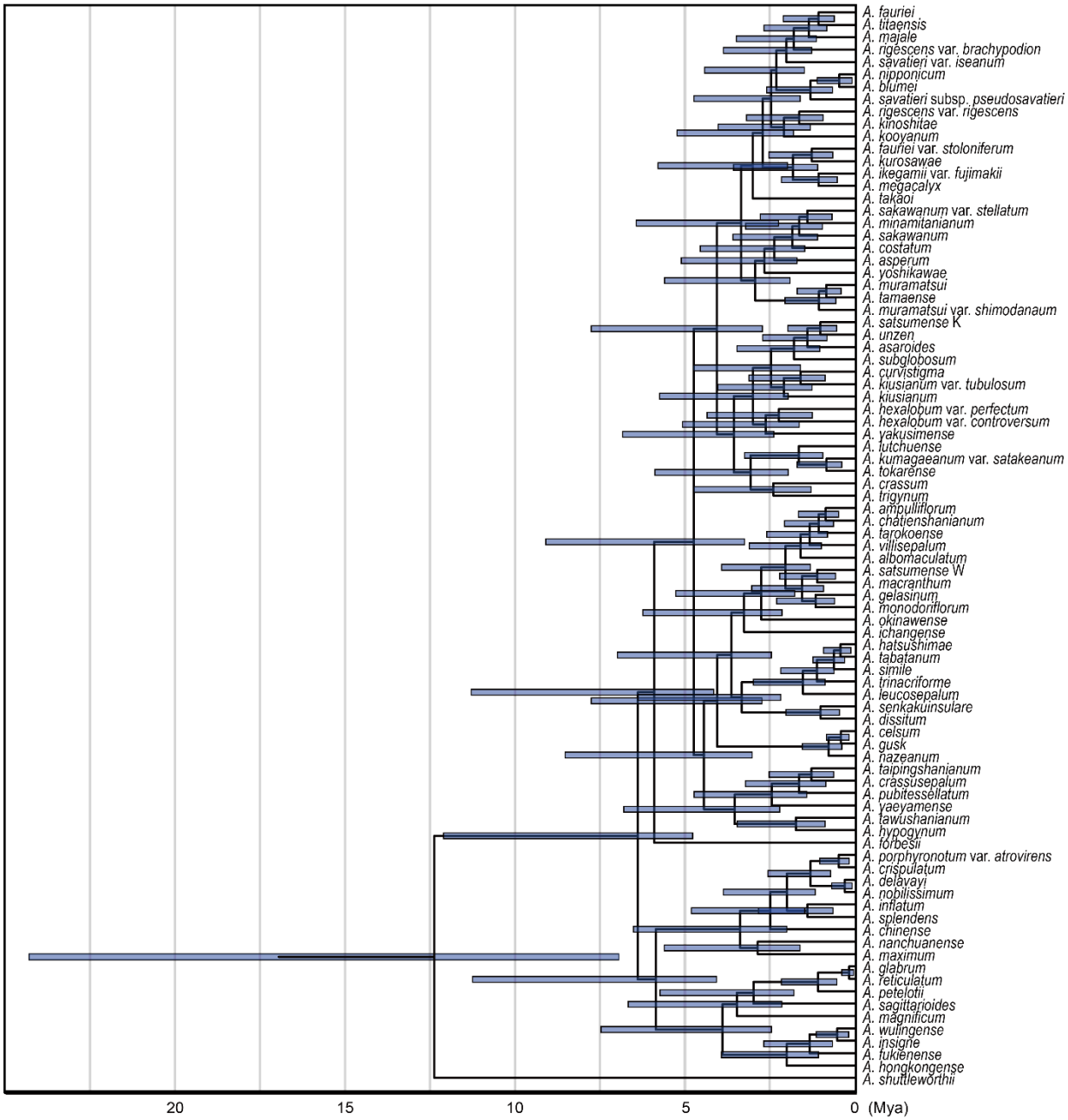

Fig. S4. A majority-rule consensus tree inferred from Bayesian analysis of ddRAD-seq data (50% genotyped data) showing the divergence times of major nodes and 95% highest posterior density (HPD) intervals.

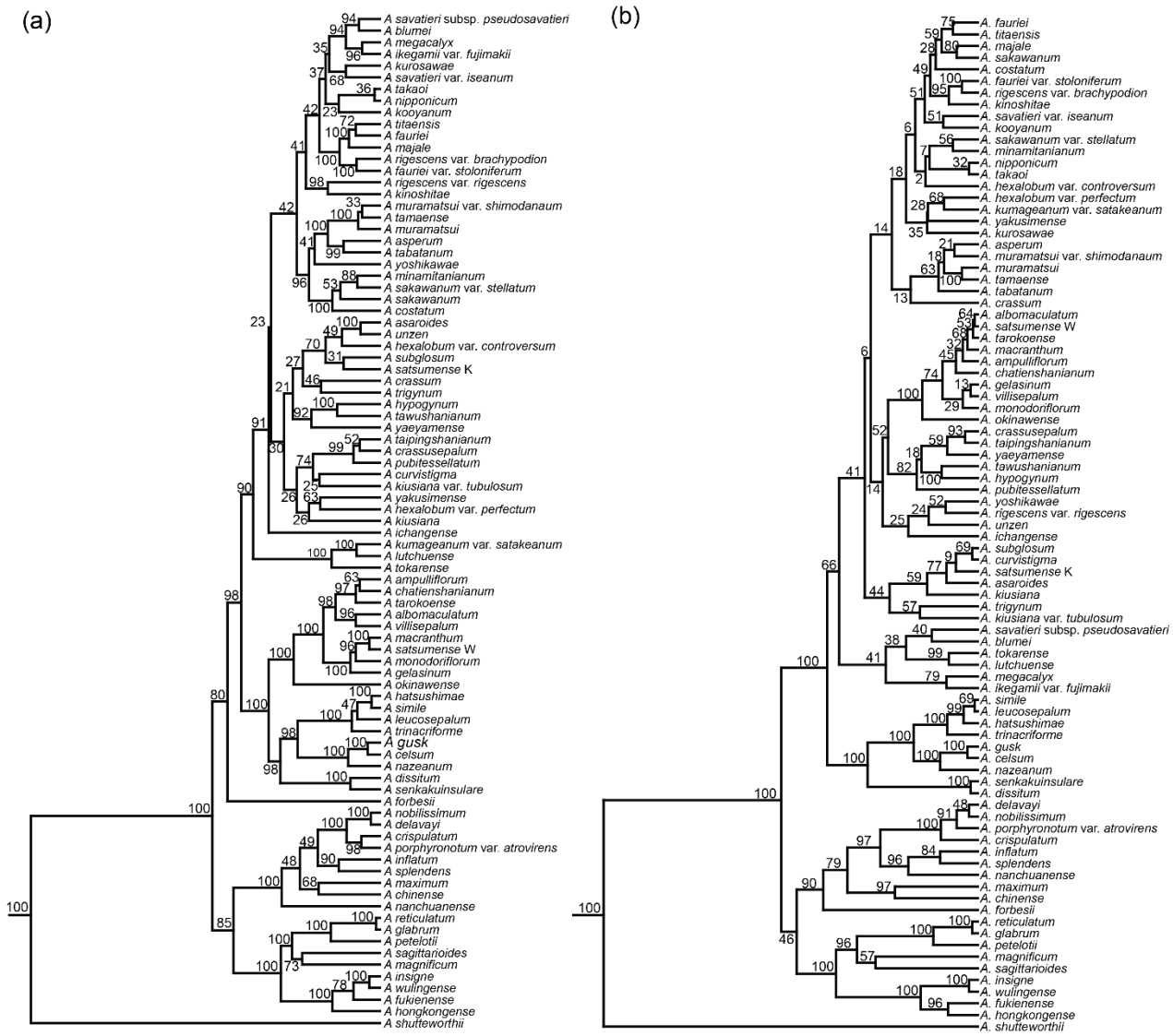

Fig. S5. Molecular phylogenetic tree of *Heterotropa* taxa estimated from Bayesian analysis using 75% genotyped (a) and 90% genotyped (b) matrices. Values above or below branches indicate the posterior probabilities of branches.

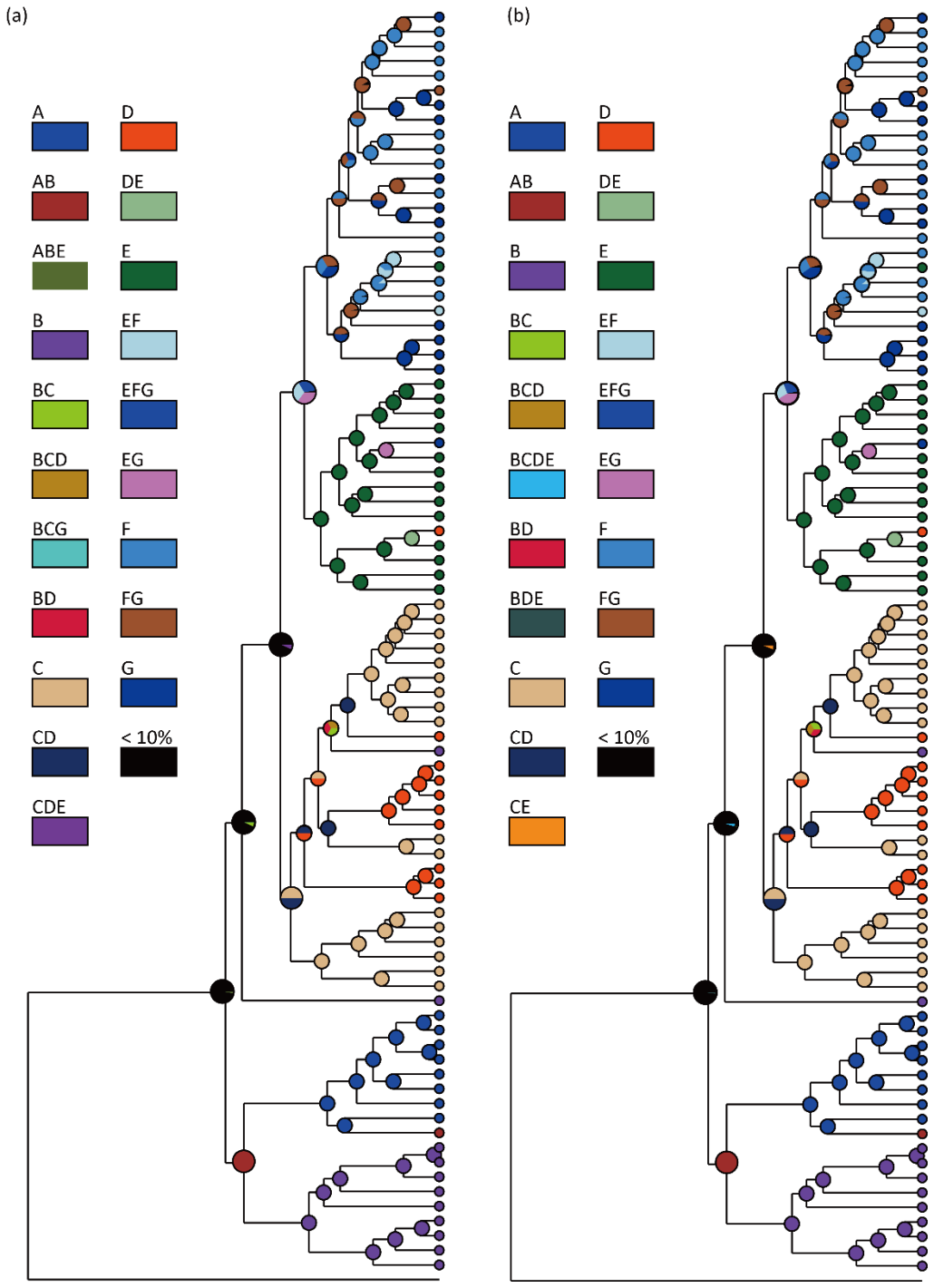

Fig. S6. The results of S-DIVA with maximum number of areas to 3 (a) and 4 (b). The colours of pie charts reflect the estimated distribution areas (A; Sichuan basin and surrounding mountains, B; other parts of mainland China, C; Taiwan and southern Ryukyu islands, D; central Ryukyu islands, E; northern Ryukyu islands and Kyushu island, F; southern part of mainland Japan including Shikoku island, and G; northern part of mainland Japan).

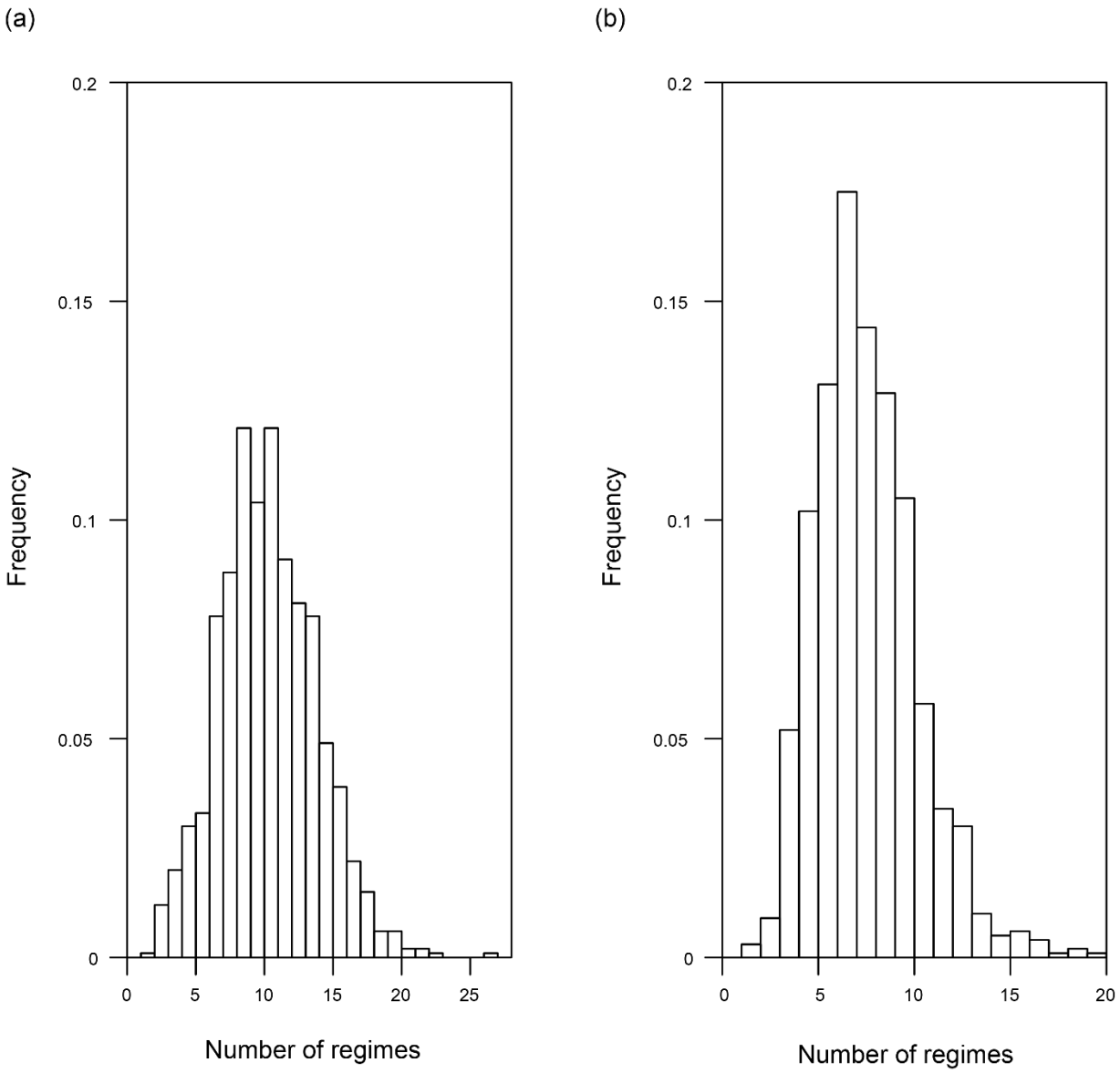

Fig. S7. Histograms of supported number of macroevolutionary rate regimes for each trait evolution; (a) flowering time and (b) calyx tube width. The number of regimes = 1 indicated there were no shifts in trait evolution rate throughout the tree.

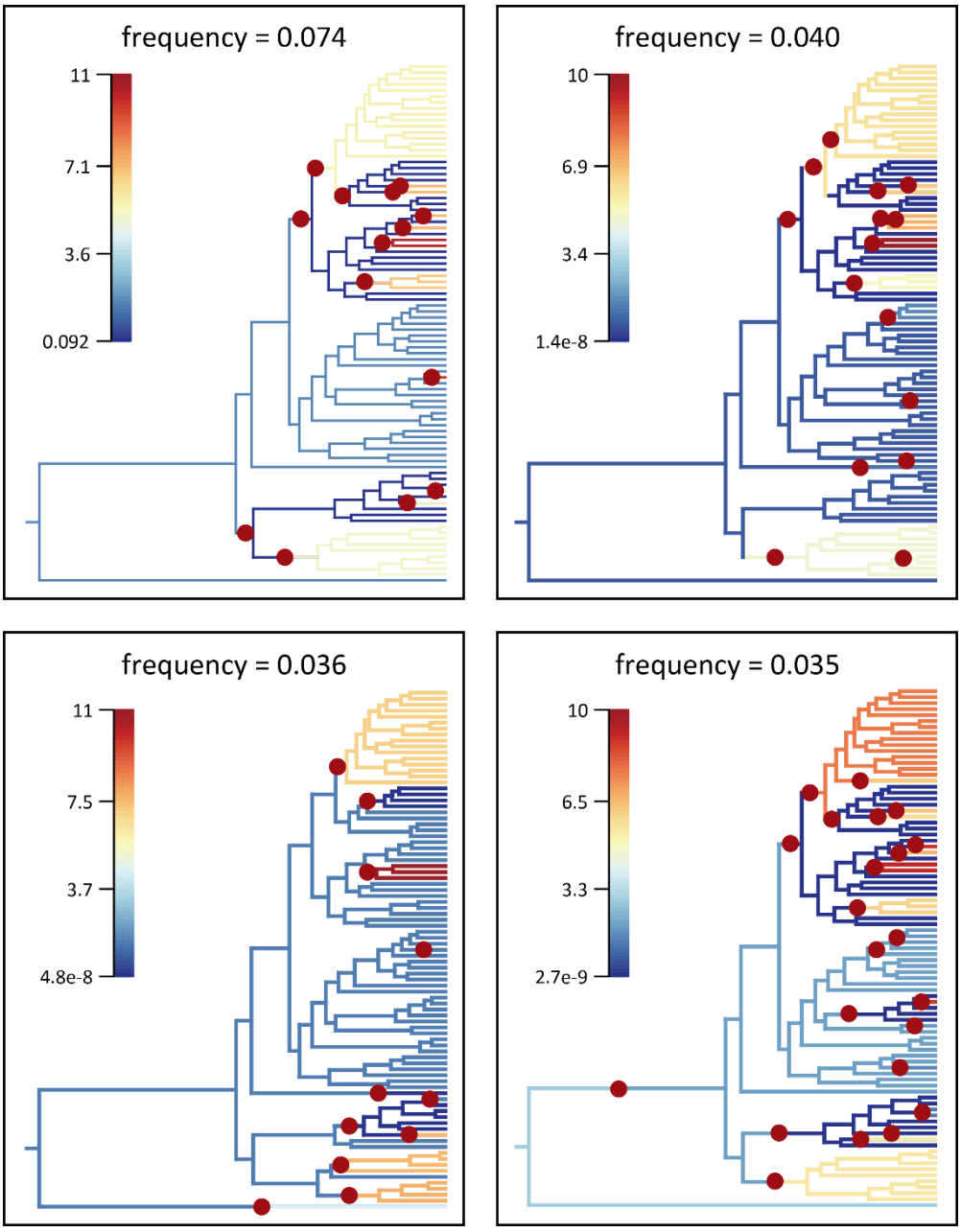

Fig, S8. The top four most credible rate shift configurations estimated by BAMM analysis using flowering time. Red circles indicate the location of rate shifts and colours of blanches are corresponded with the evolutionary rates of trait.

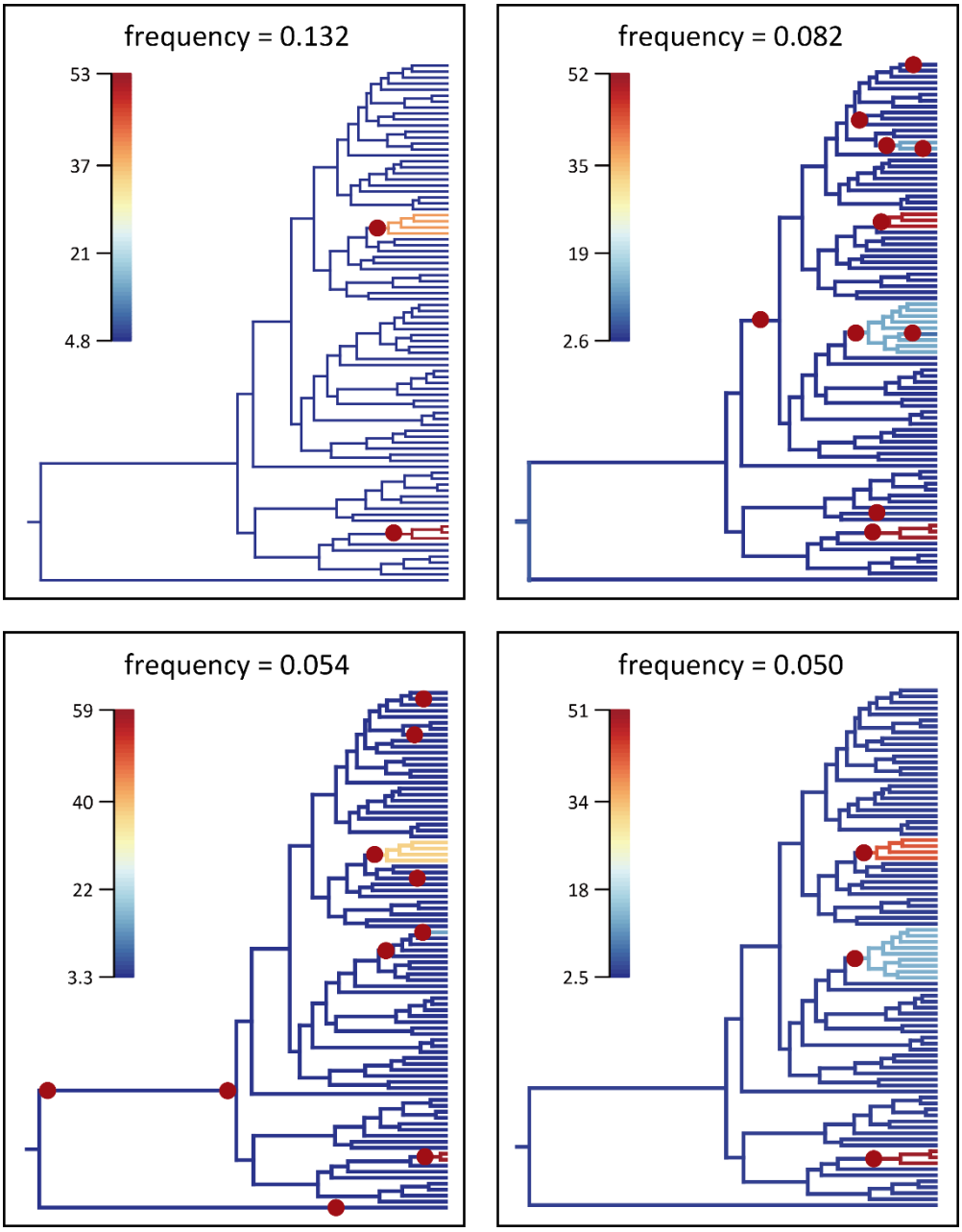

Fig, S9. The top four most credible rate shift configurations estimated by BAMM analysis using calyx tube width. Red circles indicate the location of rate shifts and colours of blanches are corresponded with the evolutionary rates of trait.

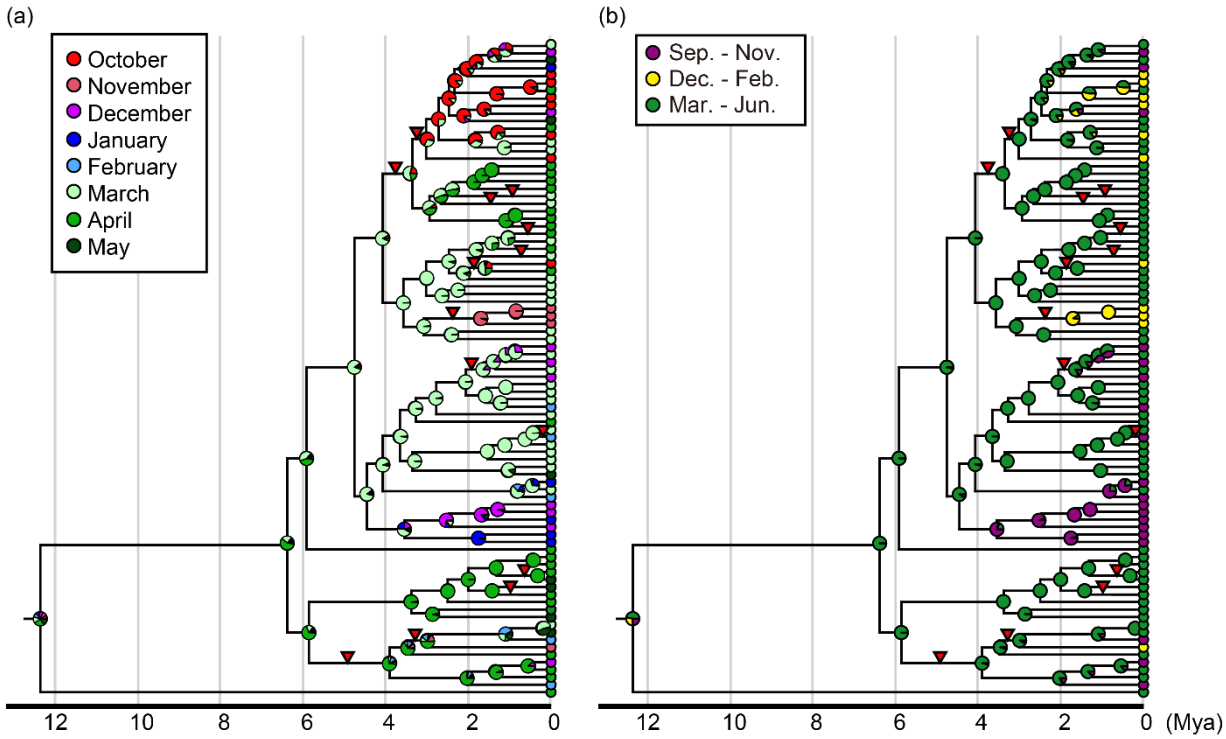

Fig. S10. The results of ancestral state reconstruction of discrete flowering times; month (a) and season (b). The topology of tree is same as Figure 1c. The red triangle represents the node where accelerated rate shift was estimated by BAMM analysis of flowering time (Fig. 2a-1).

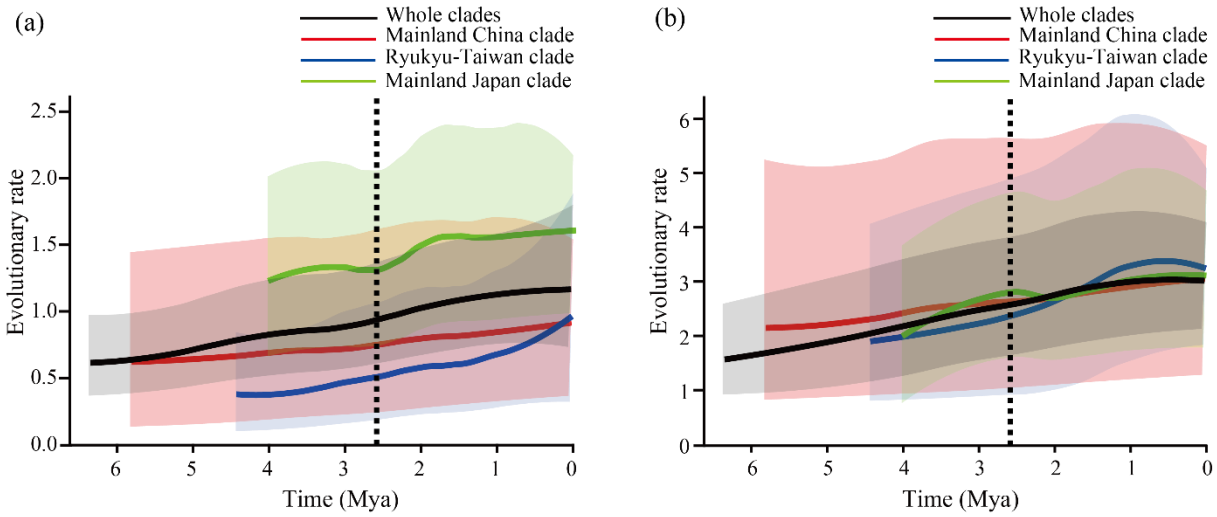

Fig. S11. The median value with 95% CI of evolutionary rate of flowering time (a) and calyx tube width (b) through time in each clade (black; whole clades, red; mainland China clade, blue; Ryukyu-Taiwan clade, and light green; mainland Japan clade). Dashed vertical lines indicate the boundary between the Pliocene and the Pleistocene (2.6 Mya).

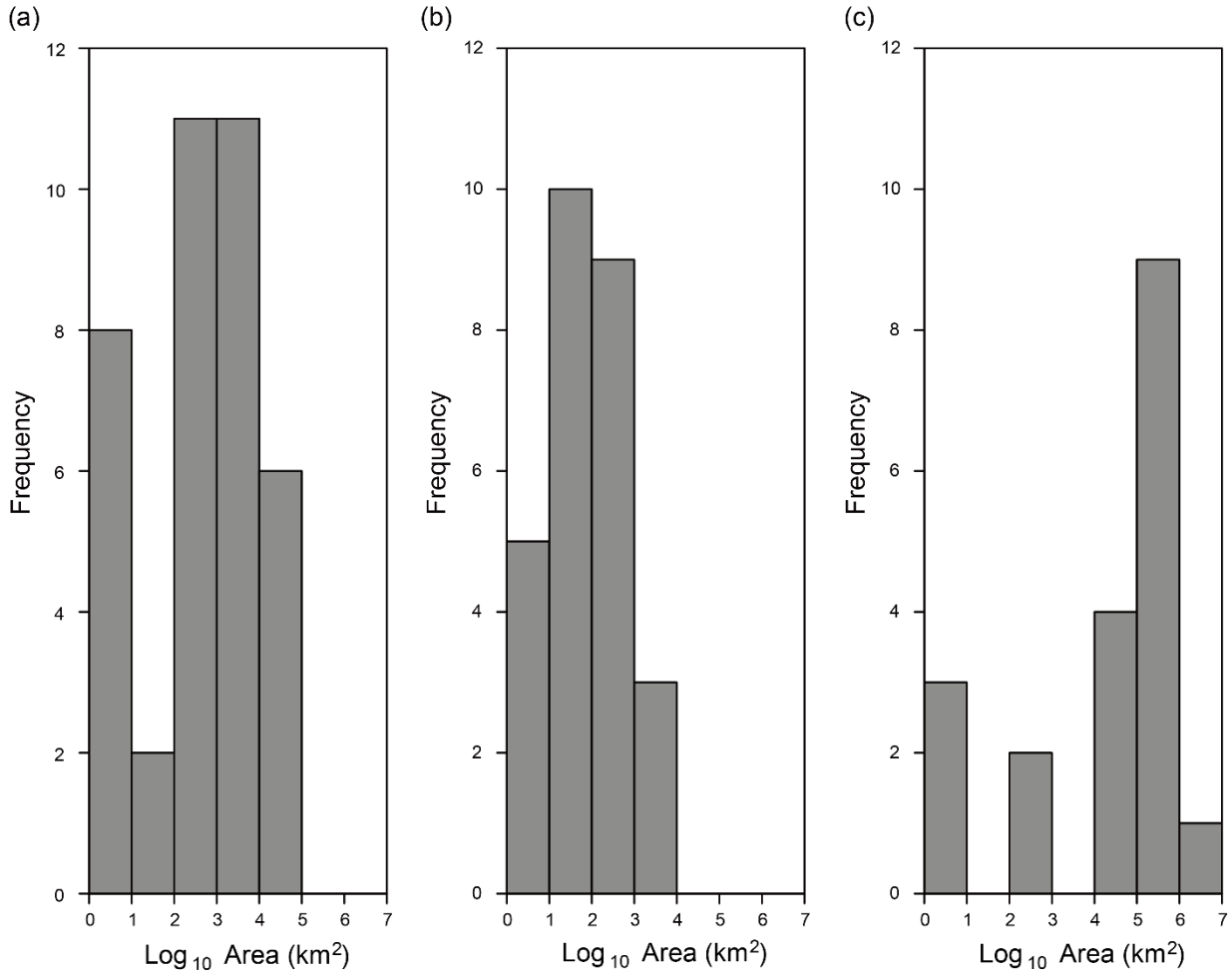

Fig. S12. Histograms of distribution area of taxa within mainland Japan clade (a), Ryukyu-Taiwan clade (b), and mainland China clade (c).

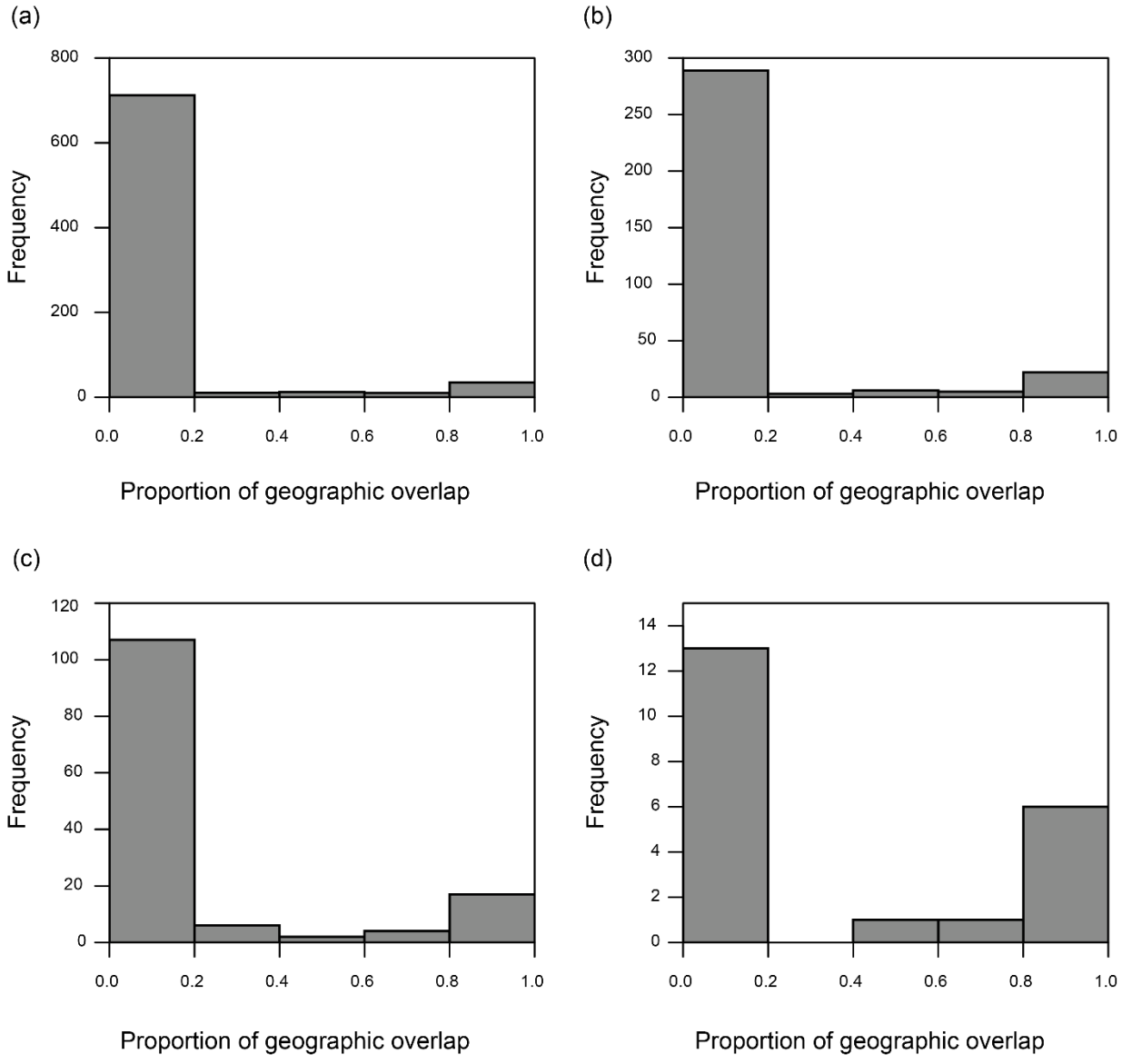

Fig. S13. Histograms of proportion of geographic range overlap between taxa pairs within mainland Japan clade (a), Ryukyu-Taiwan clade (b), mainland China clade (c), and sister-taxa pairs (d).

Table S1. Sample list used in ddRAD-seq analysis. The columns indicate the distribution region used in S-DIVA, the start and end month of flowering time, median value of calyx tube diameter (mm), distribution area calculated from the polygon formed by the distribution record(s), number of records used in the geographic analysis, the number of cleaned RAD-seq reads, and the number of loci in the 50% matrices.

Taxon name	Distribution region†	Flowering time (start month)	Flowering time (end month)	Calyx tube diameter (mm) [minimum, maximum]	Distribution Area (km^2)	No. of occurrence data	No. of RAD-seq reads	No. of loci
Asarum albomaculatum	C	12	4	11 [10, 12]	4187.34	5	1,364,347	273
Asarum ampulliflorum	C	12	3	17.5 [15, 20]	215.26	4	2,558,859	369
Asarum asaroides	E	4	5	27.5 [25, 30]	7316.76	9	1,005,898	231
Asarum asperum	E,F	3	4	9 [8, 10]	64744.28	101	1,224,717	226
Asarum blumei	G	4	5	13 [12, 14]	7352.51	24	2,252,177	335
Asarum celsum	D	1	3	10 [10, 10]	216.59	15	1,900,129	318
Asarum chinense	A	4	5	10 [10, 10]	97328.52	8	1,489,480	194
Asarum chatienshanianum	C	3	4	7.75 [7, 8.5]	639.83	9	1,810,861	311
Asarum costatum	F	4	5	10.5 [8, 13]	263.60	13	1,630,505	258
Asarum crassum	E	3	4	13 [13, 13]	3.15	1	2,051,537	349
Asarum crassusepalum	C	12	2	7 [7, 7]	60.69	6	1,275,832	241
Asarum crispulatum	A	4	4	16 [12, 20]	36720.52	5	731,042	116
Asarum curvistigma	G	10	11	11.5 [10, 13]	453.86	3	2,144,205	335
Asarum delavayi	A	4	6	15 [15, 15]	218114.79	29	1,149,735	181
Asarum dissitum	C	3	3	7.5 [7, 8]	3.15	1	1,245,668	283
Asarum fauriei	G	3	4	8.5 [7, 10]	60577.40	42	989,584	217

Table S1 continued

Asarum fauriei var. *stoloniferum*	G	4	5	9 [8, 10]	6.17	2	1,454,461	253
Asarum forbesii	B	4	5	7.5 [6, 9]	1003890.28	79	835,954	169
Asarum fukienense	B	4	6	10 [10, 10]	206959.65	53	1,052,381	173
Asarum gelasinum	C	3	4	8 [8, 8]	85.24	8	801,861	198
Asarum glabrum	B	5	6	25 [25, 25]	3.15	1	1,400,872	182
Asarum gusk	D	3	4	8.5 [8, 9]	86.64	12	1,017,556	236
Asarum hatsushimae	D	3	4	13.5 [12, 15]	11.93	4	725,731	181
Asarum hexalobum var. *controversum*	E	3	3	6 [5, 7]	6.49	2	1,037,696	268
Asarum hexalobum var. *perfectum*	E	3	4	10 [10, 10]	19172.34	16	1,241,879	267
Asarum hongkongense	B	2	5	12 [12, 12]	153.31	3	915,024	159
Asarum hypogynum	C	1	3	15 [15, 15]	123.59	7	1,738,623	311
Asarum ichangense	B	4	5	10.75 [9, 12.5]	686040.84	62	1,490,923	265
Asarum ikegamii var. *fujimakii*	G	3	4	13.5 [10, 17]	3.09	2	2,047,355	313
Asarum inflatum	A	5	5	15 [15, 15]	18648.29	12	983,274	154
Asarum insigne	B	4	5	15 [15, 15]	190239.57	40	978,225	137
Asarum kinoshitae	F	12	1	8 [7, 9]	5.92	2	987,677	213
Asarum kiusianum	E	3	4	11.5 [10, 13]	3993.44	6	1,400,694	292
Asarum kiusianum var. *tubulosum*	E	4	5	11.5 [10, 13]	619.41	3	1,288,659	250
Asarum kooyanum	F	5	6	11 [10, 12]	7610.56	9	2,755,598	317
Asarum kumageanum var. *satakeanum*	E	11	12	11 [10, 12]	95.81	4	889,370	209
Asarum kurosawae	F	10	11	13 [12, 14]	259.78	4	2,131,652	324

Table S1 continued

Asarum leucosepalum	D	3	3	8.5 [7, 10]	14.10	3	996,824	241
Asarum lutchuense	D	11	12	13.5 [12, 15]	423.87	23	1,512,018	272
Asarum macranthum	C	3	5	14 [12, 16]	5745.10	15	1,840,831	339
Asarum magnificum	B	4	5	15 [15, 15]	197314.94	17	1,205,629	210
Asarum majale	F	5	5	11 [9, 13]	150.22	6	963,832	189
Asarum maximum	A,B	4	5	17.5 [15, 20]	660193.87	31	1,033,092	181
Asarum megacalyx	G	3	5	17 [14, 20]	16232.02	16	2,622,210	363
Asarum minamitanianum	E	4	5	11.5 [10, 13]	181.61	6	548,610	119
Asarum monodoriflorum	C	2	4	9 [9, 9]	7.06	2	822,626	186
Asarum muramatsui	G	4	5	13.5 [12, 15]	442.44	9	530,240	132
Asarum muramatsui var. *shimodanaum*	G	4	5	13 [11, 15]	5.66	3	1,979,182	295
Asarum nanchuanense	A	5	5	20 [20, 20]	3.15	1	993,484	142
Asarum nazeanum	D	2	3	14 [12, 16]	3.15	1	1,277,878	246
Asarum nipponicum	F,G	10	11	10 [10, 10]	25797.62	197	280,645	84
Asarum nobilissimum	A	5	5	15 [15, 15]	-	0	1,107,813	171
Asarum okinawense	D	3	4	6.5 [6, 7]	3.15	1	1,735,621	315
Asarum petelotii	B	2	5	17.5 [15, 20]	57675.93	16	1,450,274	213
Asarum porphyronotum var. *atrovirens*	A	4	5	12.5 [11, 14]	173.40	3	1,144,066	173
Asarum pubitessellatum	C	1	5	9 [8, 10]	3.15	1	510,135	84
Asarum reticulatum	B	3	4	18 [18, 18]	3.15	1	1,468,132	201
Asarum rigescens var. *brachypodion*	F	1	3	9 [8, 10]	4121.65	33	2,103,002	346

Table S1 continued

Asarum rigescens var. *rigescens*	F	2	3	10 [10, 10]	8006.73	26	1,962,229	352
Asarum sagittarioides	B	11	4	9.5 [7, 12]	147658.26	40	1,261,660	219
Asarum sakawanum	F	4	5	10 [10, 10]	5180.45	22	2,622,795	369
Asarum sakawanum var. *stellatum*	F	4	5	10 [10, 10]	1115.98	7	656,868	145
Asarum satsumense K	E	4	5	22.5 [20, 25]	210.82	7	1,748,886	334
Asarum satsumense W	C	1	4	17.5 [14.8, 20.2]	137.83	4	841,216	181
Asarum savatieri subsp. *pseudosavatieri*	G	10	11	11 [10, 12]	373.18	3	1,704,736	250
Asarum savatieri var. *iseanum*	F	10	11	10 [10, 10]	170.51	4	1,526,335	263
Asarum senkakuinsulare	C	5	5	15 [15, 15]	3.15	1	1,756,833	296
Asarum simile	D	3	4	13.5 [12, 15]	17.07	3	1,548,706	312
Asarum splendens	A	4	5	25 [25, 25]	262763.69	65	981,268	156
Asarum subglobosum	E	3	4	13 [12, 14]	3241.28	8	483,853	92
Asarum tabatanum	D	2	3	12.5 [10, 15]	34.53	7	596,188	158
Asarum taipingshanianum	C	12	2	8.25 [6.5, 10]	42.95	5	1,148,529	202
Asarum takaoi	F	10‡	12	9.5 [7, 12]	15158.51	35	647,715	116
Asarum tamaense	G	4	5	13.5 [12, 15]	923.82	17	2,124,523	306
Asarum tarokoense	C	10	12	12 [12, 12]	129.72	3	1,318,747	264
Asarum tawushanianum	C	1	3	13.5 [12, 15]	102.69	3	1,375,473	237
Asarum titaensis	F	12	2	13 [10, 16]	3.47	2	2,066,637	312
Asarum tokarense	E	11	12	11 [10, 12]	18.62	5	1,527,639	311
Asarum trigynum	E	3	4	10 [10, 10]	22.37	4	923,350	199

Table S1 continued

Asarum trinacriforme	D	3	4	8 [6, 10]	298.16	25	1,535,333	292
Asarum unzen	E	3	4	14 [13, 15]	4202.19	7	2,459,204	362
Asarum villisepalum	C	3	5	12.5 [11, 14]	28.61	3	904,052	185
Asarum wulingense	B	12	5	12 [12, 12]	832913.59	57	1,280,655	202
Asarum yaeyamense	C	12	3	13.5 [12, 15]	2629.23	11	1,001,880	225
Asarum yakusimense	E	3	4	13.5 [12, 15]	3.15	1	1,240,300	250
Asarum yoshikawae	G	3	4	10 [8, 12]	2528.38	30	793,701	155
Asarum shuttleworthii‡	North America	5	7	27.5 [15, 40]	-	0	1,156,332	108

†A; Sichuan basin and surrounding mountains, B; other part of mainland China, C; Taiwan and southern Ryukyu islands, D; central Ryukyu islands, E; Kyushu island and northern Ryukyu islands, F; southern part of mainland Japan including Shikoku island, G; northern part of mainland Japan. ‡This value is obtained from field observation. ǂSect. *Hexastylis* taxa, used as outgroup accorrding to Takahashi and Setoguchi (2018).

Table S2. Information of newly obtained reads and chloroplast genomes of *Asarum* spp.

Taxon name	Number of raw reads	The length of chloroplast genome (bp)
Asarum macranthum	194,385	161,472
Asarun satsumense K	24,546,050	164,444
Asrum forbesii	275,687,362	164,688
Asarum wulingense	276,766	160,867
Asarum shutterwrothii	23,736,078	164,460

Table S3. The sample lists used in phylogenetic analysis of chloroplast genome.

Taxon name	Family	DDBJ accession NO.	Reference
Asarum costatum	Aristolochiaceae	AP018513	(Takahashi et al., 2018)
Asarum macranthum	Aristolochiaceae	LC529904	Newly obtained
Asarum satsumense K	Aristolochiaceae	LC529901	Newly obtained
Asarum forbesii	Aristolochiaceae	LC529900	Newly obtained
Asarum wulingense	Aristolochiaceae	LC529903	Newly obtained
Asarum shutterwrothii	Aristolochiaceae	LC529902	Newly obtained
Saruma henryi	Aristolochiaceae	NC039933	(Sinn et al., 2018)
Aristolochia tagala	Aristolochiaceae	NC041455	(Li, X et al., 2019)
Aristolochia contorta	Aristolochiaceae	NC036152	(Zhao et al., 2017)
Drimys granadensis	Winteraceae	DQ887676	(Chai et al., 2006)
Cinnamomum camphora	Laulaceae	MH050970	(Wu et al., 2019)
Chimonanthus praecox	Laulaceae	NC042744	(Zhao et al., 2019)
Machilus balansae	Laulaceae	KT348517	(Song et al., 2015)
Liriodendron chinense	Magnoliaceae	NC030504	(Li, B et al., 2016)
Magnolia sinostellata	Magnoliaceae	NC039941	(Yao et al., 2018)
Sarcandra glabra	Chloranthaceae	MH939147	(Han et al., 2018)
Chloranthus japonicus	Chloranthaceae	KP256024	(Sun et al., 2016)